The Effects of Chronic Elevated Temperatures on Potato (*Solanum tuberosum* L.) Tuber Development

by

Abigail Mia Guillemette

A thesis submitted to the Graduate Faculty of
Auburn University
in partial fulfillment of the
requirements for the Degree of
Master's of Biological Sciences

Auburn, Alabama
May 6, 2023

Climate change, crop physiology, abiotic stress, heat stress, phytohormones, gene expression, transcriptomics, potato, *S. tuberosum*

Approved by

Dr. Aaron Rashotte, Co-Chair, Professor and GPO, Department of Biological Sciences
Dr. Courtney Leisner, Co-Chair, Assistant Professor, Department of Biological Sciences
Dr. Daniel Jones, Committee Member, Assistant Professor, Department of Biological Sciences

Abstract

With global temperatures rising due to climate change, many crops are being adversely affected. Potato (*Solanum tuberosum* L.) is the fourth most important food crop in the world and is especially vulnerable to heat stress, facing significant yield loss when exposed to temperatures higher than 28°C. Many studies have attempted to understand this effect of heat stress on potato, but the exact mechanisms behind this inhibition remain unknown. It is understood that the environmental conditions potatoes experience during the growing period have significant impacts on the tuberization process, as signals initiated in leaves integrate environmental and circadian factors to determine the timing of tuberization. However, very few studies have examined the effects of heat stress on tubers throughout varying stages of development. A FLOWERING-LOCUS T (FT) homolog in potato, referred to as StSP6A, controls tuberization and is known to be downregulated under heat stress, contributing to the decrease in sucrose synthesis, transport, and ultimate crop yield loss. Previous studies have found an important role of SP6A in tuber initiation, but results suggest that other genes are responsible for the continued growth of tubers. Significant knowledge gaps remain in our understanding of the genes responsible for tuberization signaling, especially under the context of elevated temperature. This study uses whole-plant physiology, transcriptomics, and hormone profiling to gain insight into the molecular mechanisms behind heat stress impacts on potato tuber development.

Acknowledgments

First and foremost, I would like to thank my advisors, Dr. Aaron Rashotte and Dr. Courtney Leisner, who led me through every step of my project and who balanced each other out in ways that make me feel very fortunate to have been mentored by both. I'm incredibly lucky to have had twice the amount of support and guidance throughout my studies than most, and I couldn't have chosen one over the other. I'd also like to thank Dr. Daniel Jones, the third person in my committee and in our small plant people group in the Department of Biological Sciences. If I were to compare Courtney and Aaron as my mom and dad in an analogy, Daniel would've been the cool uncle, and he did an excellent job of playing the role throughout my studies. Thank you to everyone in both of my labs that have helped me, especially to Collin Modelski from the Leisner lab and Mary Durstock who was in a completely different department than me but who I couldn't have completed my experiment without. I'd also like to thank Risheek Khanna from the Rashotte lab and Natalie Powers, an undergraduate in the Leisner lab who is now graduated and doing great things; you all offered a tremendous amount of help during my experiment. And of course, thank you to the rest of the people in the Rashotte and Leisner labs and the Capitulab. I am truly lucky to have worked with such an incredible group of plant people.

I'd like to thank my collaborators in the Czech Republic who provided a novel part of my research through phytohormone analyses, and especially to Eva Pokorna who was always so hospitable in our email conversations. Thank you to Coffee Mafia for supplying me with unlimited caffeine and for being my queer oasis in a college town of football fans, and to my trailer park for offering me a reprieve from the bumbling college life of downtown Auburn. I'd also like to thank my parents, my brother, and friends in Huntsville that offered me as much support as they could from a distance, as my first time in a new town by myself proved to be not

easy. And thank you to Kayla Wilson, an old friend and graduate student from my undergraduate research lab who helped me get settled here as an Auburn alumni and resident. A special thanks to my cat, Pusa, for keeping me company and giving emotional support cuddles, and to my partner, Drew, for the endless support both from a distance and by my side.

My time here at Auburn has proven to be the most challenging yet rewarding time of my life so far, and I truly appreciate everyone who helped me bring my dream to fruition. I couldn't have done it without you!

Table of Contents

List of Tables

List of Figures

List of Abbreviations

AmbT	Ambient Temperature
ElevT	Elevated Temperature
TI	Tuber Initial
IMT	Intermediate Tuber
MAT	Mature Tuber
SP6A	SELF PRUNING 6A
CO_2	Carbon Dioxide
ROS	Reactive Oxygen Species
HSF	Heat Shock Factor
HSP	Heat Shock Protein
ABA	Abscisic Acid
FT	FLOWERING LOCUS T
TAC	Tuberigen Activation Complex
PEBP	Phosphatidylethanolamine83 Binding Proteins
SES	SUPPRESSING EXPRESSION OF SP6A
CEN	TERMINAL FLOWER 1/CENTRIONALIS
COL1	CONSTANS-like1
IT1	IDENTITY OF TUBER 1
GA	Gibberellic Acid
JA	Jasmonic Acid
TOC1	TIMING OF CAB EXPRESSION 1

A	Carbon Assimilation
g_s	Stomatal Conductance
FW	Fresh Weight
DW	Dry Weight
PE	Paired-End
GO	Gene Ontology
TPM	Transcript Per Million
IAA	Indole-3 Acetic Acid
OxIAA	Oxo-Indole-3 Acetic Acid
SA	Salicylic Acid
RNA-Seq	RNA-Sequencing
PCA	Principal Component Analysis
DEG	Differentially Expressed Gene
TFL	Terminal Flower

Chapter 1: Introduction

Climate Change and its Impacts on Crop Production

Since the industrial revolution in the late 1800's, anthropogenic carbon dioxide (CO_2) emissions have steadily increased, leading to unprecedented levels of global atmospheric CO_2 levels. Being a greenhouse gas that traps energy from solar radiation, these increasing CO_2 levels have contributed to a consistent rise in average global temperatures by approximately 1.1°C since the late 1800's. Unless CO_2 emissions are substantially reduced or stopped, global surface temperatures are expected to continue rising by an additional 1.5-8°C by next century (IPCC, 2021). These changes are expected to occur disparately across regions, with some areas (especially those of extreme latitudes) likely to experience more rapid and dramatic increases in temperature.

Higher-than-optimum temperatures are known to affect and interfere with biological processes of all living organisms, disturbing everything from biochemical functions to whole-organism development and physiology. In plants, several changes can occur under heat stress, including changes in respiration and photosynthetic efficiency, injuries such as leaf and stem scorching, and growth inhibition (Bita and Gerats 2013). At the cellular level, heat stress can cause reactive oxygen species (ROS) production leading to cellular damage, changes in cell wall composition and fluidity, inhibition of proteins synthesis, and denaturing/degradation of proteins and other important molecules (Zhu et al. 2021; Bita and Gerats 2013). Heat stress can also induce changes in hormone expression leading to shortened plant life span/premature senescence (Sade et al. 2018). All these mentioned effects contribute to decreased plant productivity.

As sessile organisms unable to escape unfavorable conditions, plants have evolved ways to cope with heat stress, particularly through expression of heat shock factors (HSFs) (Guo et al.

2016). HSFs are transcription factors that subsequently activate the expression of other genes such as heat shock proteins (HSPs) that assist in rescuing molecular functions (Guo et al. 2016; Janni et al. 2020). HSPs chaperone and stabilize the folding of other proteins, allowing them to stay in their functional conformation in the face of high temperatures (Janni et al. 2020). Additionally, hormone signaling is an important player in stress response; for example, abscisic acids (ABA) responds to oxidative stress caused by ROS, triggering the expression of transcription factors (Li et al. 2020). Recently, small RNAs such as microRNAs (miRNA) and small interfering RNAs (siRNA) have also been shown to play important regulatory roles in stress response by moderating gene expression either transcriptionally or post-transcriptionally (Zuo et al. 2021). In response to heat stress, these molecules can modulate gene expression related to many plant processes including flowering, auxin signaling, and ROS scavenging (Zuo et al. 2021).

Despite these adaptations allowing plants to survive unfavorable temperatures, they can still accumulate physiological changes such as decreased/abnormal reproduction, altered growth and development, and increased susceptibility to disease (Hatfield and Prueger 2015; Leisner et al. 2022). In agriculturally important plants, this can mean significantly decreased crop yield and therefore less food and resources. Crop production worldwide is already facing adverse effects from climate change as plants struggle to acclimate to unfavorable conditions, and the projected increase in temperatures will only exacerbate these issues (Dahal et al. 2019). It is predicted for climate change to decrease crop production by 17–24% by next century (Dutta et al. 2022). To ensure global food security, it is imperative we develop stress-tolerant crops to keep up with the changes in climate we expect to see in the coming decades.

There has been considerable research in recent years on understanding how plants cope with climatic stress and potential methods of breeding resistance. One popular method of study is through growing plants in growth chambers; with these, humidity, temperature, light intensity and cycling, and even ambient levels of gasses such as CO_2 can be controlled, providing a powerful tool for controlled plant studies. Chosen conditions for growth chamber experiments vary greatly across studies on heat stress in plants, with some using static temperatures that change only between nighttime and daytime, and others ramping temperatures throughout day/night cycles or even throughout growing seasons (Hancock et al. 2014; Leisner et al. 2017). Furthermore, some studies use future climate projections as growing conditions to better understand how plants will respond to expected climate conditions. A recent study has found the choice of different climate projections to substantially impact the outcome of experiments (Leisner et al. 2017). To represent the most accurate projection of future climate on potato production, the present study uses a climate projection for the mid-twenty-first century, dynamically downscaled for a high potato-production region, to study the effects of future temperatures on potato growth.

Potato Consumption and Cultivation

Potato is the fourth most important food crop after wheat, maize, and rice with a global production of 360 million metric tons in 2020 (Birch et al. 2012; FAO 2023). Ranked as one of the most efficient crops in terms of dry matter and protein production per hectare, potato is considered a staple in many countries, with the top producers being China, India, Russia, USA, and Ukraine (Mäck and Schjoerring 2002; Zaheer and Akhtar 2016). In recent years, potato production has increased significantly in developing countries, with roughly half of total

production occurring in Asia (de Haan and Rodriguez 2016). Millions of people depend on it for survival, as it is easy to grow and is rich in dietary fiber, vitamins, and minerals (Beals 2019). In addition to its role in food security, potato is economically important in many countries; in the United States alone, potato production reached over $3.6 billion USD in 2021 (NASS 2021). Besides use as a fresh vegetable, it is also used in the production of processed foods such as potato chips, starch, alcohol, and animal feed (de Haan and Rodriguez 2016; Sprenger et al. 2016).

Modern cultivated potato (*Solanum tuberosum* L.) was domesticated from wild *Solanum* species native to the Andes mountains in Peru, and today they are clonally propagated through their tubers. Potato seeds are rarely or never used for cultivation. Due to a likely autopolyploidization event of early landrace diploids (*S. tuberosum* groups Stenotomum and Phureja), modern potato cultivars have tetraploid genomes (*S. tuberosum* group Andigena), which presents difficulties for breeding efforts (Hardigan et al. 2017). Additionally, clonally propagated crops are more susceptible to inbreeding depression as deleterious mutations tend to accumulate quickly through asexual reproduction (Zhang et al. 2019). Their germplasm and breeding efforts are often maintained through tissue culture, where both traditional breeding methods and newer breeding methods such as clustered regularly interspaced short palindromic repeats/CRISPR associated 9 (CRISPR/Cas9), transcription activator-like effector nucleases (TALENs) and zinc-finger nucleases (ZFNs) are used (Hameed et al. 2018). Most breeding efforts in potato work towards developing cultivars that produce higher yields, longer storage times, and higher processing quality (Hameed et al. 2018).

Tuber Development and Signaling

Unlike other tuberous vegetables, potatoes are not root-derived; instead, the tuber of a potato develops from a stolon, or underground stem, originating from axillary buds at the base of the main stem. These tubers store carbohydrates, lipids, and protein reserves, and they serve as a vegetative means of reproduction for potato plants as the axillary buds or "eyes" produce sprouts with the ability to grow into new plants after a period of dormancy (Zierer et al. 2021). The development of a stolon into a tuber is caused by changes in the carbohydrate metabolism of the plant in response to environmental cues and internal signaling, and the process is characterized by several stages: tuber initiation, filling, and maturation (Obidiegwu et al. 2015). During tuber initiation, the stolon apical tip ceases elongation and begins radial cell expansion and division, driven by the transport and deposition of sucrose synthesized in the leaves during photosynthesis (Zierer et al. 2021). Sucrose and other metabolite deposition in the stolon continues throughout the filling stage until the tuber reaches maturity, after which the tuber enters a dormancy phase for a period of time. During dormancy, protease inhibitor genes in tubers are upregulated, attenuating proteolysis and the remobilization of resources, which in turn prevents the tuber from sprouting (Weeda et al. 2009).

The initiation and continued development of tubers is mediated by complex interactions between molecular signals including proteins, phytohormones, and RNAs (Dutt et al. 2017). The most notable gene responsible for regulating tuberization is SELF-PRUNING 6A (StSP6A), a FLOWERING LOCUS T (FT) homolog and mobile protein that induces sucrose transport from the leaves to tubers (Navarro et al. 2011). During tuber initiation, SP6A forms a complex in the stolon tips with FT-like proteins StFDL1a and StFDL1b, facilitated by interactions with 14-3-3 proteins, a group of plant proteins that regulate interactions and binding between other proteins

(Teo et al. 2017). This complex has been named the tuberigen activation complex (TAC) after the florigen activation complex (FAC) described in rice (Teo et al. 2017). The terms florigen and tuberigen refer to mobile signals produced in the leaves that induce flowering and tuberization, respectively (Teo et al. 2017). While integrated in TAC, SP6A directly interacts with sucrose transporters such as StSUT4 and SUGAR WILL EVENTUALLY BE EXPORTED (SWEET) transporters and induces a switch from apoplastic to symplastic transport, leading to sucrose deposition in the stolons (Abelenda et al. 2019). SP6A is part of the PHOSPHATIDYLETHANOLAMINE83 BINDING PROTEINS (PEBP) family along with 14 other genes related to flowering/tuberization, including inhibitors of SP6A called SP5G-A and SP5G-B (Zhang et al. 2021a).

SP6A is regulated by many other molecules (Figure 1) including transcription factors and small RNAs. A transcription factor of the BEL1-like family, BEL5, and microRNA (miRNA)172 promote SP6A transcript expression, while a FT-like miRNA SP5G and miRNA156 inhibit StSP6A (Abelenda et al. 2016; Dutt et al. 2017). TAC can be inhibited by TERMINAL FLOWER-1 (TFL1) or StCEN, another gene in the PEBP family (Zhang et al. 2020). A thermo-sensitive miRNA named SUPPRESSING EXPRESSION OF SP6A (SES) has also been found to target StSP6A, indicating that post-transcriptional regulation is important for regulation of the tuberigen, especially in early stages of growth (Lehretz et al. 2019; Park et al. 2022). Initiation of the tuberization process is also dependent on the perception of environmental cues, namely light intensity, photoperiod, and temperature (Kondhare et al. 2021). Most grown cultivars induce tuber formation under short-day (SD) photoperiods. This process is controlled by a suite of circadian clock genes, including a CONSTANS-like gene (StCOL1) (Hoopes et al. 2022). Under long-day, COL1 is upregulated and directly activates SP5G, a direct inhibitor of

SP6A, which in turn inhibits tuberization (Abelenda et al. 2016). Recently, other genes controlling tuber formation have been discovered: a gene called IDENTITY OF TUBER (IT1) was discovered to be responsible for the differentiation of stolons into tubers (Tang et al. 2022). Knockout mutants of this gene in *S. tuberosum* produced stolons but no tubers (Tang et al. 2022).

Hormone signaling also plays a role in potato tuber development. Previous work has shown gibberellic acids (GA), cytokinins, ABA, jasmonic acid (JA) and auxins are key regulators of tuberization. GAs have long been attributed to tuber inhibition as they promote the elongation of stolons rather than radial growth (Xu et al. 1998). At the induction of tuber growth, GA levels within the stolon tips are reduced through expression of GA oxidase genes, allowing for lateral cell division resulting in tuber development (Kloosterman et al. 2007). It is thought that SP6A plays a role in regulating the expression of GA 2-oxidase genes (Park et al. 2022). ABA also plays a significant role in potato development, mainly through antagonistic action to GA, as lower GA:ABA levels promote tuber growth (Xu et al. 1998; Chen et al. 2022). Cytokinins promote tuberization by activating cell division and facilitating starch accumulation in cells, while auxins, especially indole-3-acetic acid (IAA), play a pivotal role in the differentiation of stolon tips to tubers (Pathak and Upadhyaya 2021). A higher cytokinin to auxin ratio specifically promotes tuberization and increases yield (Hannapel et al. 2004). Additionally, JAs are more recently discovered to play a role in tuberization by facilitating the radial expansion of tuber cells (Hannapel et al. 2004; Singh et al. 2020).

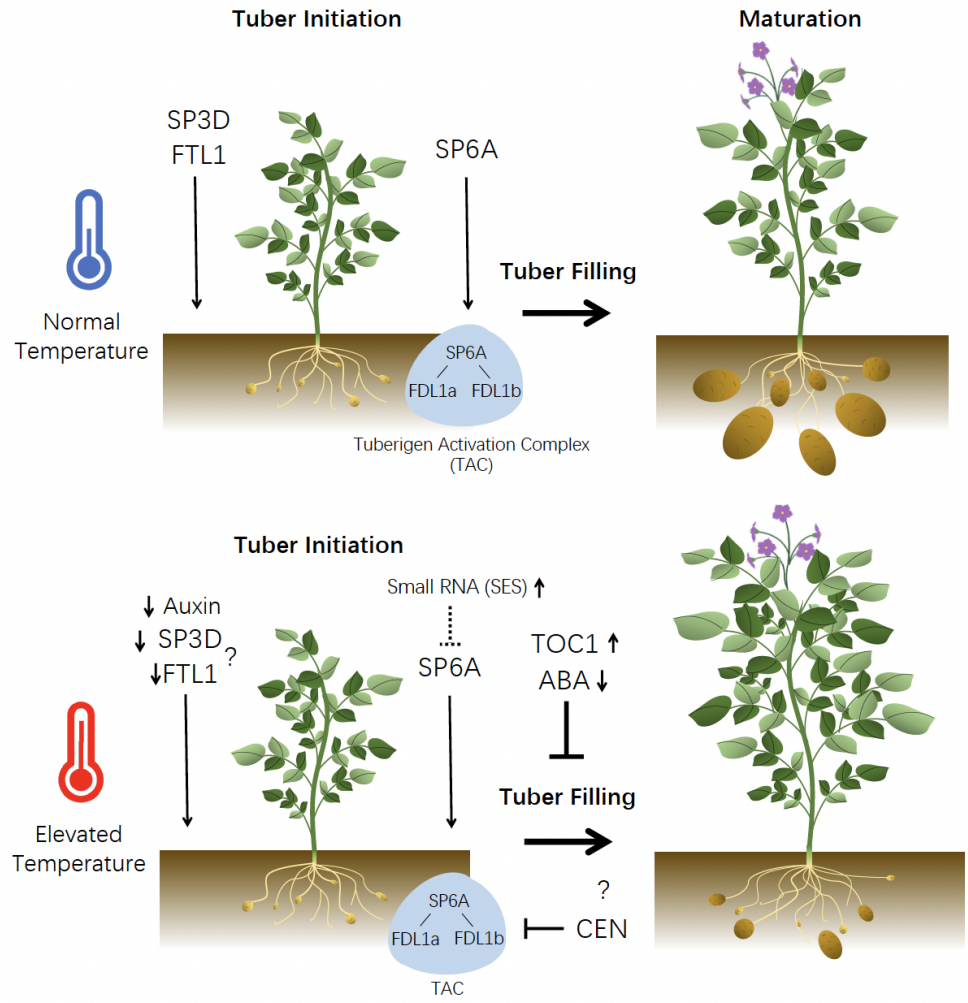

Figure 1. Model for known and potential changes in gene expression and hormone levels under elevated temperature. Lines with arrows indicate movement, while lines with closed ends indicate inhibition. Dashed lines with closed ends indicate partial inhibition. Small arrows indicate increases or decreases in expression under elevated temperature. Question marks indicate potential regulators of tuberization under elevated temperature. SP3D, SELF PRUNING 3D; FTL1, FLOWERING LOCUS T-like; SES, SUPPRESSING EXPRESSION OF SP6; SP6A, SELF PRUNING 6A; TOC1, TIMING OF CAB EXPRESSION 1; ABA, Abscisic Acid; CEN, CENTRIONALIS/TERMINAL FLOWER 1; FDL1a, & b, FD-like 1a & b.

Effects of Heat Stress on Potato

Descending from wild potatoes native to the temperate climate of the Andes mountains, *S. tuberosum* is especially susceptible to heat stress, with optimal temperatures for tuber growth being 14-22°C (Van Dam et al. 1996). High temperatures cause a range of physiological and

developmental defects in tubers including irregular heat sprouts from axillary buds, tuber chaining in which axillary buds on a tuber grow stolons that develop into other tubers, deformed/undesirably shaped tubers, "russeting" or cracking of skin, and even internal necrosis (Zhang et al. 2021b; Robinson et al. 2020; Ginzberg et al. 2009; Sterrett et al. 1991). It can also cause early postharvest dormancy break, decreasing winter storage times for production (Zhang et al. 2021b). One of the more concerning effects, however, is the significant loss of tuber yield under heat stress. Potato plants grown under elevated temperatures experience a shift in biomass allocation towards the aboveground plant, leading to longer stems, more leaves, and decreased tuber yield (Tang et al. 2018). Even under moderately elevated temperatures (≥25°C), a significant decrease in potato yield is observed (Dahal et al. 2019; Hancock et al. 2014). Although the degree of this response varies among potato cultivars, even relatively heat-tolerant cultivars experience significant yield loss (Tang et al. 2018; Rykaczewska 2013). This effect has been found to be exacerbated the earlier in development the heat stress occurs (Rykaczewska 2015). Considering the expected increases in global surface temperatures in coming decades, this loss in potato yield poses a substantial threat to food security.

The exact mechanisms that cause lower tuber yield under heat stress is not yet completely understood and is an area of considerable research in recent years. Some studies have attributed this effect to impaired photosynthesis under elevated temperatures and therefore less photoassimilate production (Wolf et al. 1990; Timlin et al. 2006). However, more recent studies provide conflicting evidence on whether elevated temperatures negatively affect photosynthesis in potato plants; some studies report no change or even positive effects on photosynthesis rates (Park et al. 2022; Hancock et al. 2014; Singh et al. 2015). In terms of chlorophyll content, there is also inconsistent evidence on the effects of temperature, with some studies reporting increased

levels, some reporting decreased levels, and others reporting changes in chlorophyll a/b ratios under high temperatures (Hancock et al. 2014; Tang et al. 2018; Sing et al. 2015). Variation in these results may be due to differences among cultivars and environmental conditions used. Additionally, since most studies report larger aboveground biomass of heat-stressed plants, it is more likely that tuber yield is due to changes in signaling and transport rather than a lack of photoassimilates (Tang et al. 2018).

Under heat stress, it is known that SP6A is inhibited post-transcriptionally in earlier stages of tuberization, while transcriptional regulation is more important in later stages (Park et al. 2022). In early stages of tuberization, SP6A is inhibited through RNA based-interference by a small RNA called Suppressing expression of SP6A (SES), causing less sucrose transport to the stolons and suppressing tuberization (Lehretz et al. 2019). In StSP6A over-expression lines, tuber numbers (initiated tubers) were rescued, indicating an important role in tuber formation/differentiation, but yield (growth) was still significantly decreased under high temperatures (Park et al. 2022). Furthermore, delayed tuberization is seen even in instances where SP6A expression is not affected (Park et al. 2022). This indicates that SP6A plays a significant role in tuber formation, but there are other genes responsible for the continued growth and development of tubers to maturity. Another transcriptional inhibitor of SP6A, a circadian clock gene called TIMING OF CAB EXPRESSION (StTOC1), is known to have increased expression in tubers under elevated temperatures (Morris et al. 2019; Hancock et al. 2014). Antisense transgenic lines with decreased expression of TOC1 displayed a significant increase in both aboveground biomass and tuber yield compared to wild type under high temperatures, while overexpression of TOC1 significantly decreased biomass and tuber yield (Morris et al. 2019). This gene is hypothesized to contribute to transcriptional suppression of SP6A at later stages in

tuberization (Park et al. 2022). More research on this gene could offer promising results for breeding heat resistance in potatoes.

Studies investigating the effects of temperature on the COL1-SP5G inhibitory pathway have found that the circadian clock gene COL1 has increased expression under high temperatures, but SP5G expression is not affected or is even lower in stolons under higher temperatures (Park et al. 2022; Morris et al. 2019). As STCOL1 directly upregulates SP5G, this suggests that the StCOL1-SP5G inhibitory photoperiod pathway is separate from the thermo-regulatory pathway (Park et al. 2022).

Despite recent developments in understanding the effects of heat stress on potato yield, the exact molecular mechanisms remain unknown, and there are many genes involved that have yet to be explored. It is estimated that climate change has the potential to reduce potato production by up to 18-32% by next century, greatly threatening both the potato industry and global food security (Hijmans 2003). Although many factors of climate change may affect potato production, temperature fluctuations and heat stress remain among the most uncontrollable factors (Singh et al. 2020). Breeding heat-resistant potato cultivars is an imperative goal for coping with climate change with research on the topic gaining momentum in recent years. Most studies attempting to identify the mechanisms associated with temperature impacts on tuberization exposed potato plants to acute heat stress and took measurements only at final harvest, at the end of the tuberization process. Very few studies to date have observed developing tubers under chronic heat stress. This study investigates the mechanisms behind heat-induced yield loss in potato plants using a whole-plant approach, observing physiological and molecular changes of both source and sink tissue over time. Physiological aspects of the plant such as photosynthetic efficiency, senescence, and chlorophyll levels of leaves were examined,

and final aboveground biomass and tuber yield were collected at the end of the growing period. Additionally, RNA expression and endogenous hormone content of both leaves and tubers at different developmental stages were examined. The objectives of this study are to understand the molecular mechanisms behind yield loss of potato plants grown under heat stress and to find candidate genes for breeding heat resistance in potatoes. The effects of elevated temperature on tuber development are highly complex, and heat resistance in potatoes is likely polygenic (Hancock et al. 2014). Understanding the key mechanisms behind this process requires more in-depth studies of physiology, development, and molecular interactions to preserve potato production in the face of climate change.

Chapter 2: Methods, Results, and Discussion

Growth Chamber Experiment

Potato plants were grown in controlled growth chambers using Conviron Adaptis chambers under ambient (AmbT) and elevated temperature (ElevT) conditions (n = 2). Seed tubers of the chip-processing cultivar Manistee were obtained from Michigan State University, courtesy of Dr. Dave Douches, and stored at room temperature for 3 weeks to break dormancy. Sprouted seed tubers were cut into halves and planted in 14.2L pots with Promix BX soil. Plants were grown either in the elevated temperature conditions predicted for the mid-21st century (2040-2060) or in conditions that represent the average temperature from 1980 to 2000 (the established control climate period; Leisner et al. 2017) (Supplementary Material 1). The projected temperatures were downscaled for Eau Claire, Michigan, as this region is a major producer of potatoes in the Midwest (Leisner et al. 2017). The *CRCM_cgcm3* climate model from the Leisner et al. (2017)

study was chosen since it had the highest temperatures occurring during the initiation and filling phases of tuberization, which was shown to have the largest effect on tuber yield. Maximum and minimum temperatures along with photoperiod changed every two weeks to mimic seasonal fluctuations during mid-May to mid-September (Figure 2; Supplementary Material 1). The aim was to use realistic, dynamic temperatures that potato plants would normally experience during the length of a growing period rather than using static temperatures. Light intensity was measured at the top of the canopy using a LI-180 spectrometer and ranged from 300-500μmol m^{-2} s^{-1}, and height was adjusted every 2 weeks (LICOR Biosciences, Lincoln, NE, USA). Relative humidity was set to 60% in all chambers. Initially, all plants were watered equally twice a week with 1L of water per plant until 60d, after which the plants were watered 2-3 times a week according to soil moisture. Each chamber was fertilized with ~14g Jack's Classic All Purpose 20-20-20 Fertilizer diluted in 7L of water once a week once sprouts emerged, about two weeks after planting (JR Peters Inc., Allentown, PA, USA). The plants were rotated twice a week across chambers of the same treatment to ensure uniform light distribution. Two or four plants were sampled at four time points every 30 days after planting during the growing period (two plants at 30 and 90d, and four plants at 60 and 120d). Plant samples within the same chambers were pooled together, and each chamber counted as a biological replicate (n = 2). Leaf samples were collected and immediately flash frozen in liquid nitrogen. Tubers were collected and categorized into 3 different developmental classes based on weight before flash frozen: Tuber Initials (TI) (<0.6g), Intermediate Tubers (IMT) (0.6-5g), and Mature Tubers (MAT) (>5g) (Supplementary Figure 1). Tissue samples were stored at -80°C and ground into a fine powder to use for RNA extraction and hormone expression analysis.

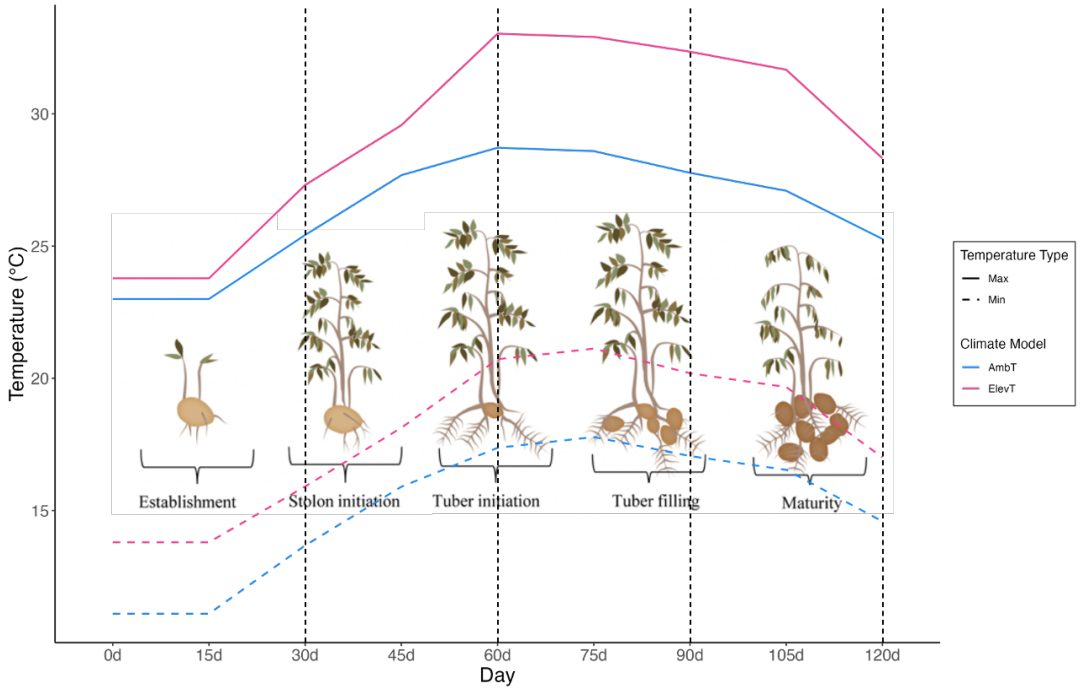

Figure 2. Maximum and minimum temperatures of the ambient (1980-2000) and elevated (2040-2060) climate models over the 120-day growing period. Vertical dashed lines indicate sampling dates. Image of the potato plant growth stages is taken from Obidiegwu et al. (2015).

Photosynthetic Efficiency, Chlorophyll, Biomass, and Final Yield

Gas exchange of the leaves was recorded *in situ* between 11:00 and 13:00 to determine photosynthetic CO_2 assimilation (A) and stomatal conductance (g_s) using a LI-6400 portable photosynthesis system (LICOR Biosciences, Lincoln, NE, USA). Temperature, relative humidity, CO_2 concentration, and light intensity of the LICOR were set to mimic the ambient conditions within the growth chambers. Following gas exchange measurements, two fresh leaves from each sampled plant were collected for photosystem II efficiency analysis through dark-induced senescence. Four 6mm diameter leaf discs were taken from the fresh leaves collected from each chamber, placed adaxial side up on 3mM MES, and blocked from all exposure to light. Photosystem II efficiency was measured through chlorophyll fluorescence via F*v*/F*m* at 24, 48, 72, and 96h as described by Zwack et al. (2016). After 4 days, each leaf disc was then

transferred to 500µl of 100% methanol overnight, and a UV/Vis spectrophotometer was used to measure total chlorophyll of the methanol extract for each leaf disc as described by Zwack et al. (2016) (Beckman Coulter, USA). Total chlorophyll was measured for 60, 90, and 120d old leaves.

After 120 days, plant height was taken by measuring the tallest point of each plant. The entire aboveground plant was cut off, and fresh weight (FW) was recorded before placing the plants in a 60°C dryer for 2 weeks to measure dry weight (DW). Tubers were collected fresh and counted per chamber, and final yield per chamber was taken by weighing the collective mass of all tubers with a mass greater than 0.6g (tuber initials were excluded from final yield). T-tests, ANOVA, and Tukey post-hoc tests on all physiology data were completed using the *stats* R package (R Core Team, 2022).

Phytohormone Extraction and Analysis

Samples from 90d and 120d collection days were used for the phytohormone analysis with three technical replicates per sample. Between 10-20mg of frozen ground tissue powder were placed into microtubes and lyophilized overnight in a FreeZone 1 freeze dry system at -50°C (LabConco, Kansas City, MO, USA). Phytohormone determination was done in the Laboratory of Hormonal Regulations in Plants, Institute of Experimental Botany of the Czech Academy of Sciences as previously described in Prerostova et al. (2021). Homogenized samples (ca. 1.5-2mg DW) were extracted with 100µL 1M formic acid solution. Mixtures of stable isotope-labeled phytohormone standards were added at 1pmol per sample. The extracts were centrifuged at 30,000×g for 25min at 4°C. The supernatants were applied to SPE Oasis HLB 96-well column plates (10mg/well; Waters, Milford, MA, USA) conditioned with 100µL acetonitrile and 100µL

1M formic acid using Pressure+ 96 manifold (Biotage, Uppsala, Sweden). After washing wells three times with 100µL water, the samples were eluted with 100µL 50% acetonitrile in water. An aliquot of the extract was analyzed on a liquid chromatography/mass spectrometry (LC/MS) system consisting of UHPLC 1290 Infinity II (Agilent, Santa Clara, CA, USA) coupled to 6495 Triple Quadrupole Mass Spectrometer (Agilent, Santa Clara, CA, USA), operating in MRM mode, with quantification by the isotope dilution method. Data acquisition and processing was performed with Mass Hunter software B.08 (Agilent, Santa Clara, CA, USA). The three technical replicates per sample were averaged together, and technical replicates with a relative standard deviation higher than 30% were excluded. Biological replicates were then averaged together and used in ANOVA and Tukey post-hoc tests using the R *stats* package on all metabolites unless otherwise noted (R Core Team, 2022).

RNA Extraction and Sequencing

Pooled tissue from two to four plants per chamber was used to extract total RNA using Spectrum Plant Total RNA Extraction kit (Sigma-Aldrich, St. Louis, MO, USA). The RNA was treated with Turbo DNA-free kit, and concentration and integrity were quantified using a NanoDrop Microvolume UV-Vis Spectrophotometer (Thermo Scientific, Wilmington, DE, USA) and 2100 Bioanalyzer (Agilent, Santa Clara, CA, USA). Messenger RNA was purified from total RNA using poly-T oligo-attached magnetic beads. After fragmentation, the first strand cDNA was synthesized using random hexamer primers followed by the second strand cDNA synthesis. After end repair, A-tailing, adapter ligation, size selection, amplification, and purification, quantified libraries were pooled and sequenced using sequencing-by-synthesis on Illumina Novaseq 6000 platform, producing 150-bp paired-end (PE) reads (Novogene Bioinformatics

Institute, University of California Davis, Davis, California). A total of 49 libraries were sequenced, with an average of 44,601,280 total reads (22,300,640 PE reads) per library (Supplementary Table 1).

Differential Gene Expression Analysis

RNA reads from sequencing were quality trimmed (p > 20) using *fastp* (v20), and quality checks were completed using *fastQC* (v0.11.9; Chen et al. 2018; Andrews, S. 2010). The reads were aligned to the doubled monoploid (DM) 1-3 516 R44 v6.1 *Solanum tuberosum* genome from SpudDB using *HISAT2* using default parameters (v2.2.1; Kim et al. 2019), and the alignment was annotated using the DM_1-3_516_R44_potato.v6.1.hc_gene_models.gff3 (downloaded Sept. 2022 from http://spuddb.uga.edu). Raw transcript count matrices generated from *HT-seq* (v0.13.5) using the "--stranded no" and "--order pos" options served as input for the *DEseq2* (v1.38.3) R package in which visualization, modeling, and differential expression analysis of the libraries was completed (Anders et al. 2015; Love et al. 2014). Genes with zero counts were filtered from the analysis. *P*-values were adjusted for false discovery rate using a Bonferroni correction method, and genes with *p*-adjusted values < 0.05 were considered differentially expressed. Functional annotations were downloaded from SpudDB, and additional gene ontology (GO) enrichment for differentially expressed genes was completed using *ClusterProfiler* (v4.6.0) and the TAIR database (Wu et al. 2021; Berardini et al. 2015).

Gene Coexpression Analysis

Salmon (v1.5.1; Patro et al. 2017) was used to produce transcript abundances, normalized as transcript per million (TPM) matrices for all libraries using the DM_1-

3_516_R44_potato.v6.1.hc_gene_models.cdna.fa of the v6.1 potato genome (downloaded Dec. 2022 from http://spuddb.uga.edu). TPM values were $\log_{10}$-transformed as input for the Simple Tidy gene co-expression analysis using the *Tidyverse* (v1.3.2) R package (https://github.com/cxli233/SimpleTidy_GeneCoEx; Li & Buell 2022; Wickham et al. 2019). Gene expression data was converted to z-scores, and a correlation coefficient of ≥0.8 was applied. A resolution parameter of 2 was used for clustering, then modules were filtered for containing at least 5 genes.

Results

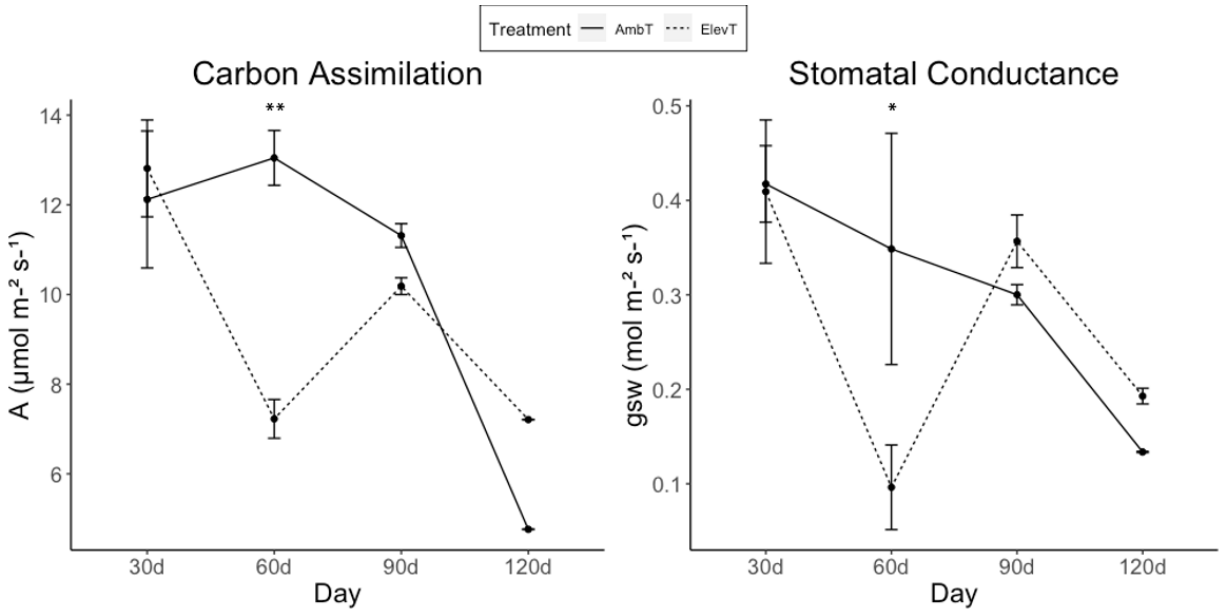

Figure 3. Carbon assimilation (*A*, measured in umol m^{-2} s^{-1}) and stomatal conductance (g_s, measured in mol m^{-2} s^{-1}) rates of plants over the 120d growing period. Error bars represent standard error between biological replicates ($n = 2$). Asterisks indicate significant differences between AmbT and ElevT from pairwise *T*-tests at each time point (* = $p < 0.05$; ** = $p < 0.01$).

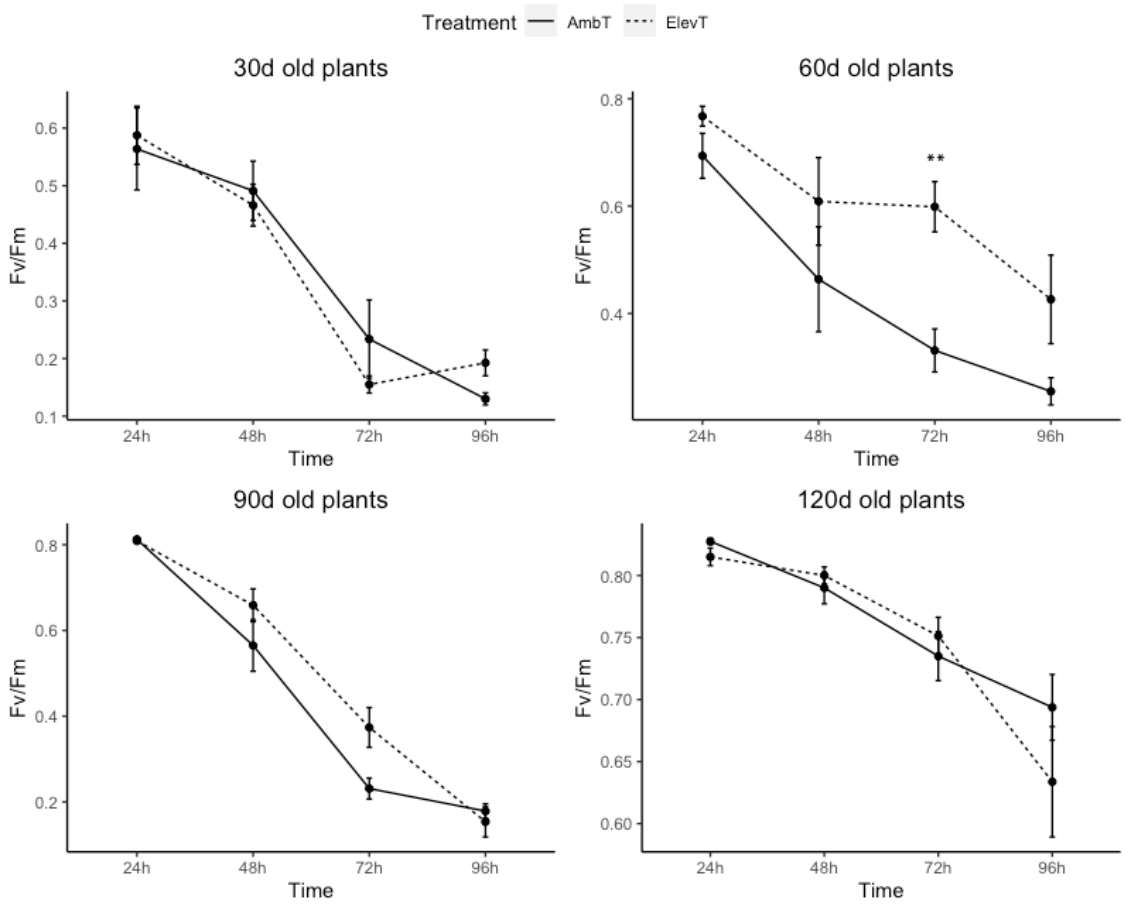

Figure 4. F*v*/F*m* measurements of leaves collected at each sampling date over the course of 96h, representing leaf senescence. Error bars are standard error between biological replicates (n=2). Asterisks indicate significant differences between AmbT and ElevT from pairwise *T*-tests at each hour of measurement (** = $p < 0.01$).

Leaf Physiology

To understand the effects of elevated temperature on potato leaf physiology, gas exchange of the youngest mature leaves was recorded in terms of carbon assimilation (A) and stomatal conductance (g_s) at each time point. Rates of gas exchange were not significantly different between treatment groups, except at 60d where the elevated temperature (ElevT) plants had significantly lower rates of both A and g_s than ambient temperature (AmbT) plants by 44.6% and 72.4%, respectively ($p < 0.02$) (Figure 3). At the beginning of the growth chamber experiment, plants from both AmbT and ElevT treatment groups were watered with equal volumes of water

per week. However, at the 60d sampling date, ElevT plants were noticed to have visibly drier soil than the AmbT plants, after which all plants were watered according to soil moisture level. This drying effect potentially occurred due to an increased rate of evapotranspiration under higher temperatures (Singh et al. 2015). However, both A and g_s rates in the ElevT plants returned to normal levels at 90d and 120d when both treatment groups were sufficiently watered, likely attributing the negative effects seen at 60d to water deficit. Similarly, there were no significant differences in senescence rates between treatment groups except at 60d, in which the ElevT plants senesced slower than the control plants and had 44.7% higher Fv/Fm measurements than AmbT leaves after 72hr ($p < 0.001$) (Figure 4). There were no significant differences in chlorophyll content between treatment groups (Supplementary Figure 2).

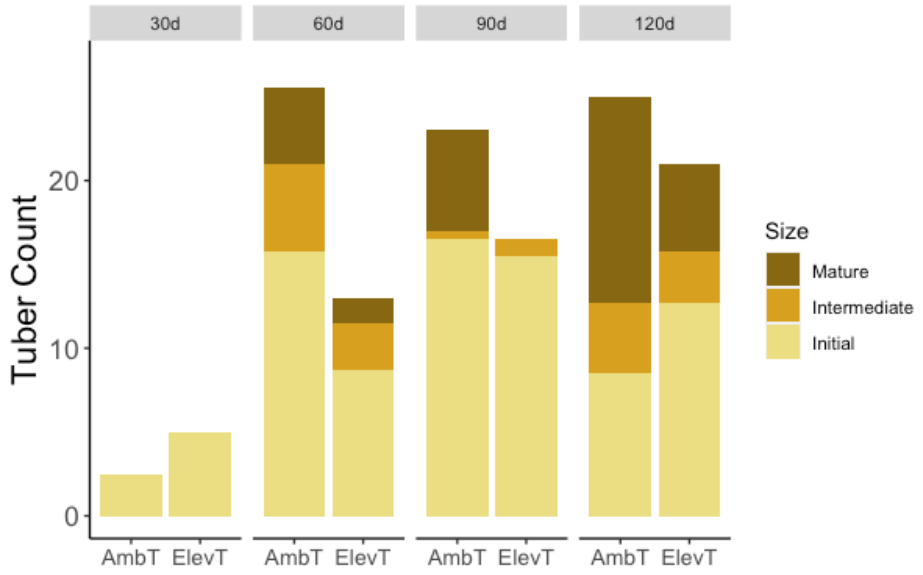

Figure 5. Stacked bar plot showing the number of each tuber size class collected at each sampling day. Counts are shown as averages per plant (from either two or four plants). Only tuber initials were collected at 30d, and no mature tubers were collected from ElevT plants at 90d. Means and standard error for each count is shown in Table 1.

	30d		60d		90d		120d	
Tuber Size	**AmbT**	**ElevT**	**AmbT**	**ElevT**	**AmbT**	**ElevT**	**AmbT**	**ElevT**
TI	1.25 ± 0.5	2.5 ± 1	7.88 ± 3.2	4.38 ± 1.1	8.25 ± 0.5	7.75 ± 2.5	4.25 ± 4.2	6.38 ± 3.2
IMT	n/a	n/a	2.62 ± 1.1	1.38 ± 1.1	0.25 ± 0.5	0.5 ± 1	2.13 ± 1.1	1.5 ± 2.1
MAT	n/a	n/a	2.25 ± 0.0	0.75 ± 1.4	3 ± 2	n/a	6.13 ± 1.1	2.63 ± 1.8*

Table 1. Mean ± standard error for average tuber counts per plant (n = 2 or 4). Asterisks indicate significant differences from the same tuber size at the corresponding time point under AmbT ($p < 0.05$).

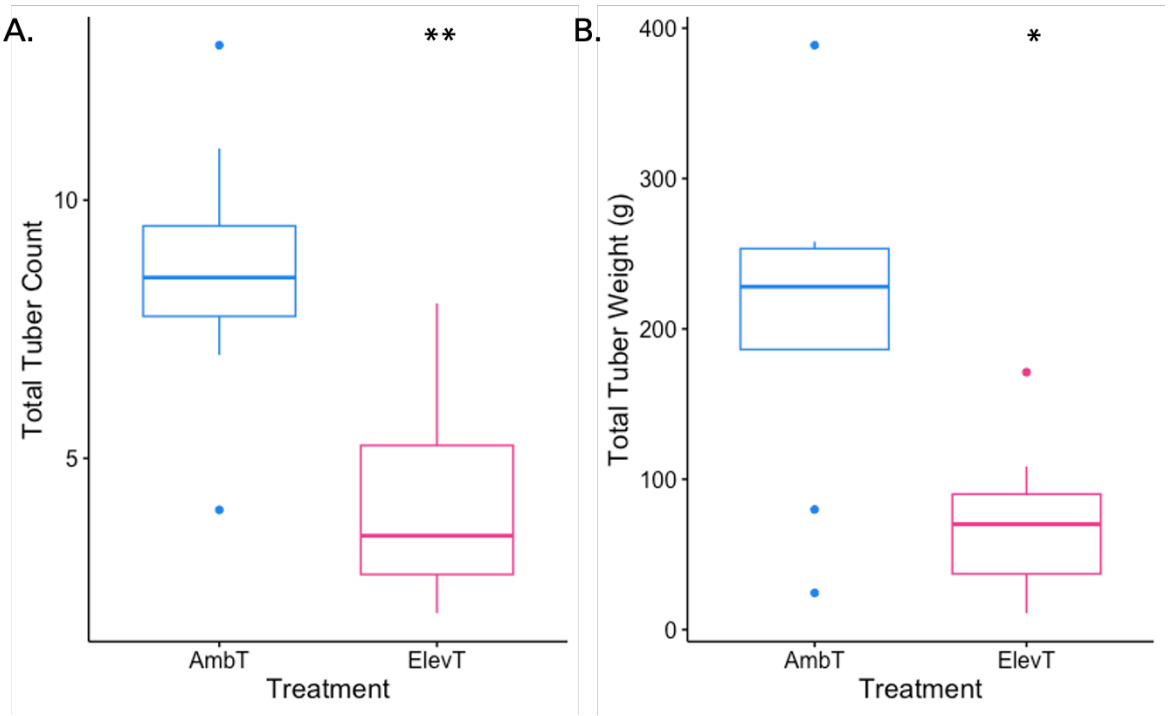

Figure 6. Box plots showing total number of tubers (A) and total tuber weight (B) of individual plants in each treatment group at 120d (n = 8). Asterisks indicate significant difference from AmbT (* = $p < 0.05$; ** = $p < 0.01$). Tuber initials were excluded from final yield measurements.

Biomass and Yield

Tuber initials (TI) were collected from all chambers at every collection time point, and intermediate tubers (IMT) and mature tubers (MAT) were collected at all sampling days except

30d (Figure 5). There were no significant differences in the number of TIs or IMTs collected between AmbT and ElevT plants, although there was a slight delay in tuber initiation, with 63 total TIs collected under AmbT vs. 35 TIs collected under ElevT at 60d ($p > 0.05$). However, at 90d, the number of TIs collected from AmbT and ElevT plants were almost equal (33 TIs vs. 31 TIs, respectively), and at 120d, 41.2% more TIs were collected from ElevT plants (51) than from AmbT plants (30) ($p > 0.05$). There were significantly less (65.8%) MATs collected in ElevT plants versus AmbT plants across all sampling time points, with a total of 79 MATs collected under AmbT and 27 MATs collected from ElevT plants ($p < 0.001$). At 60d, 18 MATs were collected from eight AmbT plants, while six MATs were collected from eight ElevT plants; however, this difference was not considered significant ($p > 0.1$). At 90d, no MATs from ElevT plants were collected, while 12 MATs were collected from four plants under AmbT ($p < 0.055$). At final harvest (120d), potato plants grown under ElevT had significantly decreased final tuber yield (both count and weight) compared to AmbT plants, with a total of 49 MATs collected from eight AmbT plants and 17 MATs collected from eight ElevT plants (65.3% decrease; $p < 0.01$) (Figure 6). AmbT plants at 120d had a mean tuber yield per plant of 210g, while ElevT plants had a mean tuber yield per plant of 72.3g (65.6% decrease; $p < 0.05$) (Fig. 6). Although the differences in plant height, aboveground FW, and aboveground DW were not significant between treatment groups ($p > 0.05$), the aboveground biomass of ElevT plants was slightly higher than AmbT plants by up to 8%, with average plant height being 37.5cm under ElevT and 34.5cm under AmbT, mean FW being 661.4g under ElevT and 638.9g under AmbT, and mean DW being 44.5g under ElevT and 41.2g under AmbT (Figure 7).

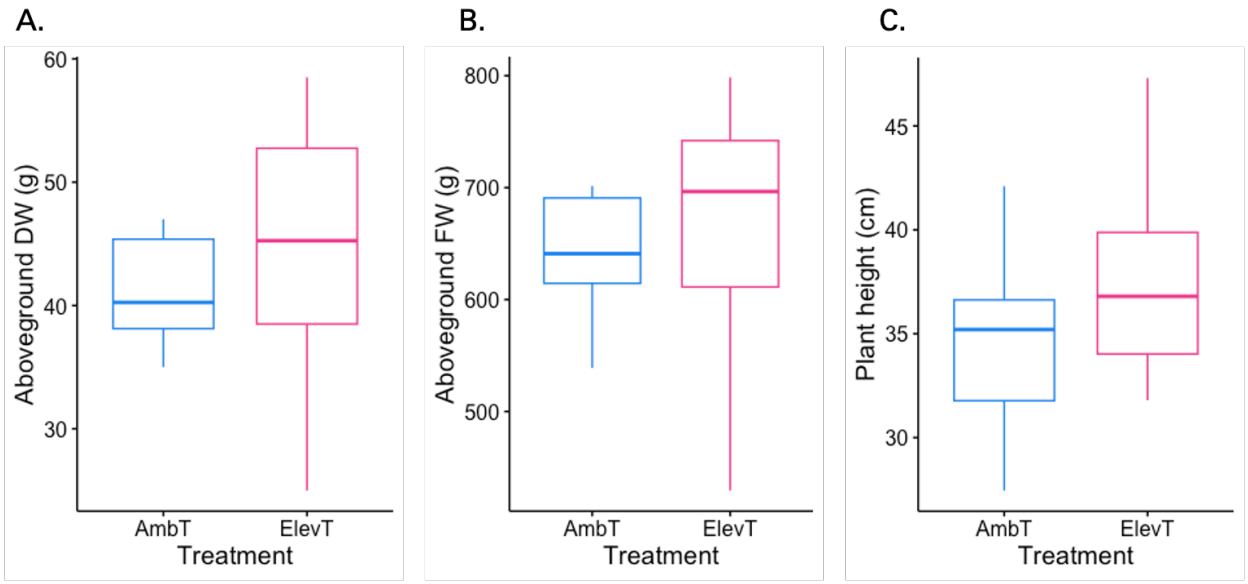

Figure 7. Box plots of aboveground plant height (cm) (A), fresh weight (g) (B), and dry weight (g) (C) of AmbT and ElevT plants collected at 120d (n = 8). There were no significant differences between treatment groups for all aboveground measurements.

Phytohormone Content

To investigate changes in signaling in potato plants grown under ElevT, we analyzed endogenous phytohormone content of all tissues using liquid chromatography and mass spectrometry (LC/MS) at the Institute of Experimental Botany of the Czech Academy of Sciences. In total, 49 phytohormone metabolites were able to be detected in measurements: 10 auxins, 23 cytokinins, 5 abscisic acids (ABA), 6 jasmonic acids (JA), and 5 other phenolic compounds including salicylic acid (SA) (Supplementary Table 2a-d). Gibberellic acids (GA) were not measured as levels were undetectable using the mentioned protocol. There were few significant differences in total levels of any hormone groups between treatment groups, although there was a significant decrease in levels of total auxins from 4,792.63pmol/gDW in ElevT leaves compared to 2,586.37pmol/gDW (46% decrease) in AmbT leaves according to Student's t-test ($p < 0.036$) (Figure 8). When specific auxin metabolites were compared, the total

difference was due to slightly lower levels of most auxin metabolites in ElevT leaves, as well as significantly lower levels of oxo-indole-3-acetic acid (OxIAA) by 54.5% ($p < 0.001$) (Fig. 8). Additionally, there were significantly higher levels of oxo-indole-3-acetic acid glucose ester (OxIAA-GE), a glucose ester conjugate of OxIAA, in both IMTs and MATs under ElevT compared to those under AmbT by up to 71.2% ($p < 0.03$). However, overall OxIAA-GE levels were quite low at < 10pmol/gDW. Both OxIAA and OxIAA-GE are inactivated forms of IAA; differences in these metabolites could be indicators of changes in active auxin levels within tissues (Pencík et al. 2013).

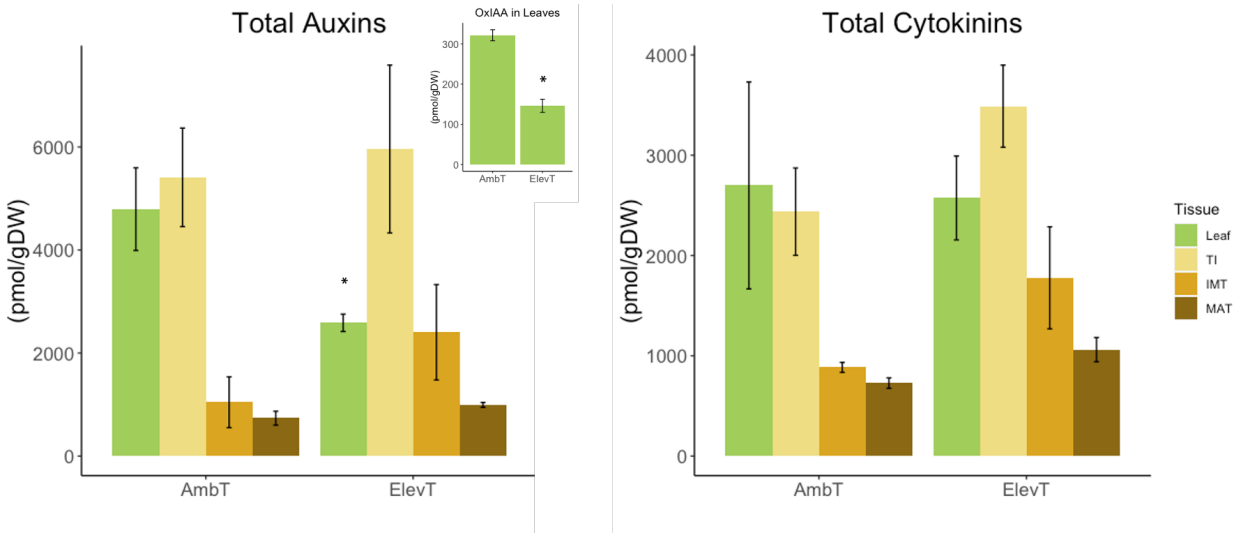

Figure 8. Total levels (pmol/gDW) of auxins and cytokinins in each tissue type. The inset graph shows levels of oxo-indole-3-acetic acid (OxIAA) in leaves between ElevT and AmbT in pmol/gDW which contributes to the significant decrease in total auxin levels seen in ElevT leaves. Asterisks indicate a significant difference from the corresponding tissue under AmbT ($p < 0.05$). Error bars are standard errors between biological replicates ($n = 2$ or 4).

Although no significant differences in total cytokinin levels between treatment groups were found, there was a trend of 30.1% higher levels of total cytokinins in ElevT TIs from 2,436.93 to 3,488.69pmol/gDW compared to AmbT ($p < 0.13$; Student's *t*-test) (Fig. 8; Table 2).

Additionally, some specific cytokinin forms were significantly affected in temperature treated samples. Both trans-zeatin riboside-O-glucoside (tZROG) and cis-zeatin riboside-O-glucoside (cZROG), O-glucoside conjugated forms of trans-zeatin and cis-zeatin, had significantly higher levels by up to 76.8% in ElevT tubers compared to AmbT tubers of all sizes ($p < 0.022$). This pattern was also seen in dihydrozeatin-7-glucoside (DZ7G), a N7-glucoside form of dihydrozeatin, with up to 81.8% decrease from 144.12pmol/gDW in AmbT to 26.2pmol/gDW in ElevT IMTs ($p < 0.005$). In MATs under ElevT compared to AmbT, there were also significantly higher levels of trans-zeatin riboside monophosphate (tZRMP) by 63.7% and cis-zeatin riboside monophosphate (cZRMP) by 48.6%, precursor forms of trans-zeatin and cis-zeatin, as well as a 67.9% increase in levels of cZRMP in ElevT IMTs compared to AmbT ($p < 0.05$). This pattern was also seen in isopentenyl adenine (iP) base form, with a 92.9% increase from 1.96pmol/gDW in MATs under AmbT compared to 27.84pmol/gDW under ElevT ($p < 0.05$). The functions of many of these altered cytokinin forms have not been thoroughly studied, especially in *S. tuberosum*, making it difficult to draw conclusions from this data. Interestingly, there was a significant increase in cytokinin methylthioderivatives (Me-CKs) in MATs under ElevT compared to AmbT, namely 2-methylthio zeatin (MeS-Z), 2-methylthio isopentenyl adenine (MeS-iP), and 2-methylthio isopentenyl adenine riboside (MeS-iPR) ($p < 0.04$). Although levels of MeS-Z and MeS-iP were quite low in most tissue types (> 1.9pmol/gDW), levels in ElevT MATs were higher by up to 97.6% compared to AmbT, with 15.01pmol/gDW of MeS-Z and 27.99pmol/gDW of MeS-iP in MATs under ElevT. MeS-iPR was also significantly affected by temperature across all tissue types, with the highest difference being an increase by 89.8% in MATs, although overall levels were low with 0.54pmol/gDW under AmbT and 5.31pmol/gDW in MATs under ElevT ($p < 0.007$). Me-CKs are exclusively synthesized through the tRNA

degradation pathway, possibly indicating changes in amino acid metabolism in potato plants under ElevT (Gibb et al. 2020).

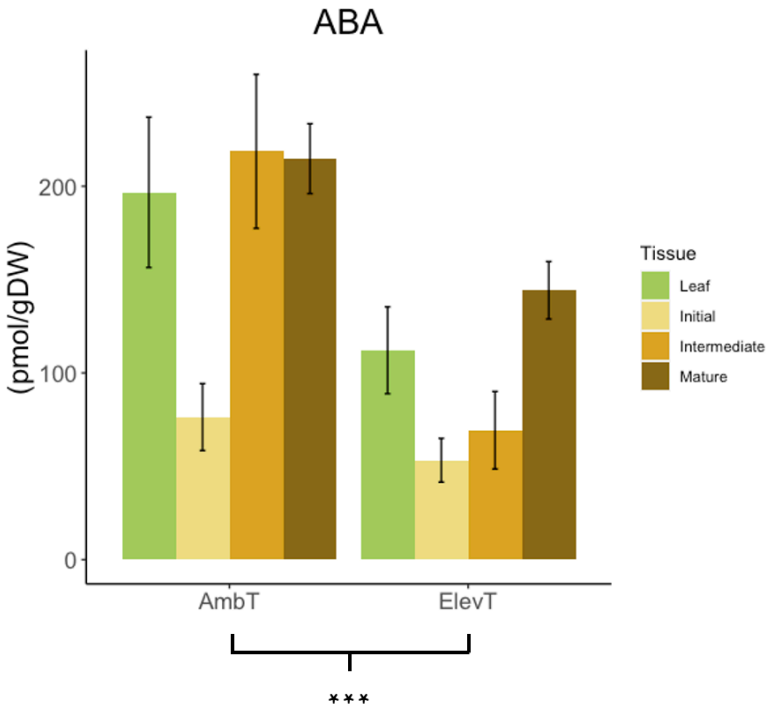

Figure 9. Endogenous levels (pmol/gDW) of ABA active form in each tissue type of 90 and 120d old plants. Error bars indicate standard error between biological replicates (n = 2 or 4). Asterisks indicate a significant difference between all AmbT and ElevT tissues ($p < 0.0001$).

ABA active form levels ranged between 53.25 - 218.67pmol/gDW across all tissues and treatments. Curiously, ABA active form levels were significantly lower in ElevT samples across all tissue types, contrary to what is known about ABA as a stress response hormone ($p < 0.001$) (Figure 9). These lower ABA levels may suggest a higher GA:ABA ratio in ElevT plants since the two metabolites are known to act antagonistically, contributing to inhibition of tuberization. Unfortunately, GA levels were below detection of measured samples, so I am unable to verify this hypothesis. The decrease in ABA levels is especially evident in IMTs with a 68.3% decrease

from 218.67pmol/gDW under AmbT to 69.34pmol/gDW under ElevT, providing a possible reason for the observed initiation of tubers but lack of maturation under ElevT.

Tissue-Treatment	Auxins	Cytokinins	ABAs	JAs	SA	Other phenolic compounds
Leaf AmbT	4,792.63 ± 802.2	2,698.46 ± 1031.2	1,757.17 ± 367.8	17,948.04 ± 11169.9	1,911.52 ± 323.8	38,298.63 ± 12236.7
Leaf ElevT	2,586.37 ± 168.9	2,573.26 ± 418	1,726.58 ± 118.1	5,760.22 ± 545.4	1,488.40 ± 272.1	22,291.83 ± 6114
TI AmbT	5,410.30 ± 956.1	2,436.93 ± 435.5	513.70 ± 125	2,302.92 ± 442.9	2,751.05 ± 941.2	30,118.42 ± 2198.9
TI ElevT	5,959.60 ± 1628.5	3,488.69 ± 409.2	679.12 ± 66.3	2,171.43 ± 316.5	3,398.65 ± 915.7	34,561.18 ± 2710.8
IMT AmbT	1,045.12 ± 492.9	884.52 ± 49.6	1,259.38 ± 211.2	1,199.77 ± 426.5	709.47 ± 349	16,252.30 ± 669.7
IMT ElevT	2,402.74 ± 925.7	1,777.40 ± 508.6	1,166.39 ± 350.1	1,504.09 ± 716.1	2,500.10 ± 1040	41,290.63 ± 20725.6
MAT AmbT	735.93 ± 135.1	727.69 ± 52.1	1,736.36 ± 42.9	689.10 ± 98.2	832.11 ± 25.1	19,026.76 ± 1247.2
MAT ElevT	993.21 ± 135.1	1,061.31 ± 120.6	2,311.00 ± 484.5	7,566.87 ± 6156.4	683.26 ± 260.6	27,615.00 ± 3649.8

Table 2. Total levels as measured by liquid chromatography and mass spectrometry (LC/MS) ± standard error of each phytohormone group in pmol/gDW. Totals are averaged by biological replicates from 90 and 120d time points for each tissue per treatment group (n = 2 or 4).

There were significantly higher total levels of phenolic compounds in MATs under ElevT compared to control by 31.1%, from 19,026.76pmol/gDW under AmbT to 27,615pmol/gDW under ElevT ($p < 0.043$; Student's t-test) (Table 2). There were also higher levels of sinapic acid (SinAc) in ElevT plants compared to AmbT across all tissue types, which was especially evident in IMTs with a 87.7% increase from 2.93pmol/gDW under AmbT to 23.75pmol/gDW under ElevT ($p < 0.003$). However, overall levels of SinAc were quite low in proportion to other phenolic compounds (< 24pmol/gDW). There was also a trend towards increased benzoic acid (BzA) levels in ElevT tubers, with the largest increase seen in IMTs by 69.6% from

10,896.61pmol/gDW under AmbT to 35,860.12pmol/gDW under ElevT. However, this difference was not significant ($p < 0.083$).

There were no significant differences in total levels of ABAs, JAs, or SA between treatment groups (Table 2). There was large variation among biological replicates as seen from the standard errors in Table 2, resulting in a lack of statistical significance between some seemingly apparent differences. Since these trends may hold upon future examination with increased replication, they are noted here. Trends found were for lower total levels of JAs in ElevT leaves by 67.9% ($p < 0.32$; Student's *t*-test) and higher levels of JAs in ElevT MATs compared to AmbT by 90.9% ($p < 0.15$; Student's *t*-test) (Table 2). There was also a trend towards higher levels of SA in IMTs under ElevT compared to AmbT by 71.6% ($p < 0.25$; Student's *t*-test), as well as higher total levels of other phenolic compounds in IMTs under ElevT compared to AmbT by 60.6% ($p < 0.36$; Student's *t*-test) (Table 2).

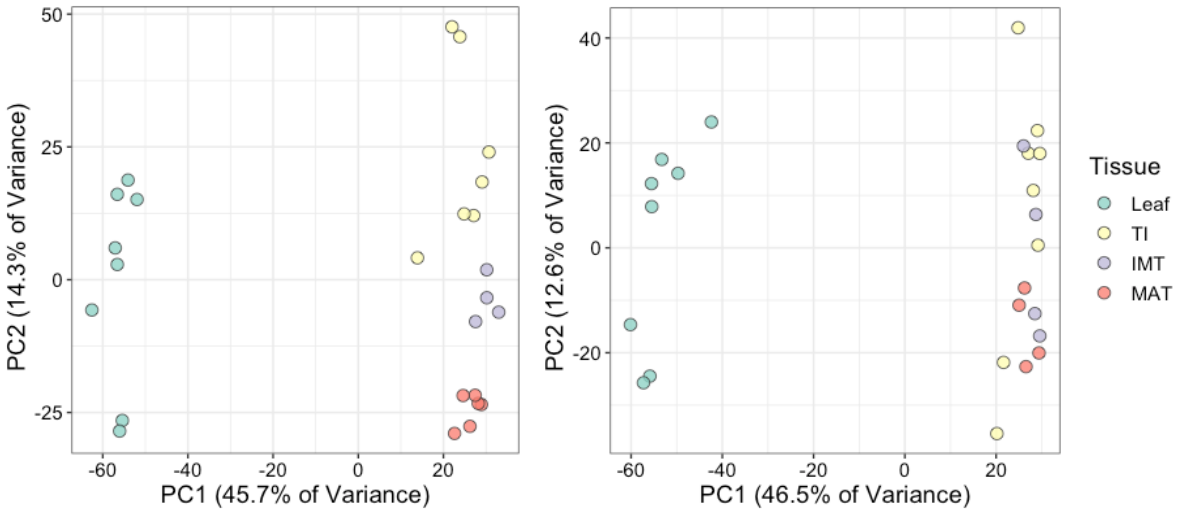

Figure 10. Principal component analysis (PCA) of all RNA-Sequencing libraries colored by tissue type for AmbT (left) and ElevT (right). Graphs were produced using *prcomp* in R.

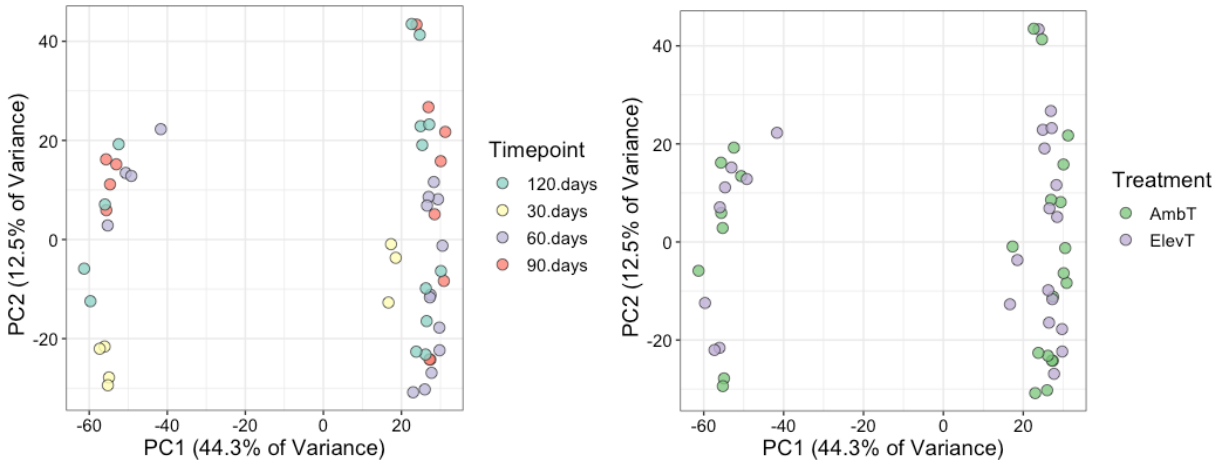

Figure 11. Principal component analysis (PCA) of all RNA-Sequencing libraries colored by time point (left) and by treatment (right). Graphs were produced using *prcomp* in R.

Global Differential Gene Expression Analysis

To examine differential expression of genes across the potato transcriptome, RNA-Sequencing (RNA-Seq) was performed on RNA extracted from all tissue samples. Following sequencing, libraries were assessed for quality and adapters were removed. Libraries were aligned to the doubled monoploid (DM) 1-3 516 R44 v6.1 *Solanum tuberosum* genome from SpudDB (http://spuddb.uga.edu) and mapping alignment statistics were assessed (Supplementary Table 1) (Pham et al. 2020). Forty five of forty-nine libraries had >75% alignment to the potato reference genome. The four libraries with low alignments all came from leaf samples. Assessment of contamination from non-plant sources was determined using BLAST (Basic Local Alignment Tool) against the NCBI non-redundant nucleotide database (nr nt), which revealed contamination with potato virus Y in the four libraries with low mapping percentages. As only mapped reads were used for subsequent analysis, these libraries were retained for differential gene expression analysis.

Principal component analysis (PCA) revealed most variation between RNA-seq libraries to be explained by tissue type, with 46% variance explained by the difference between leaves and tubers (Figure 10). When libraries were labeled by treatment and time point, there were no discernible patterns of variance between treatment groups in the PCA, and only distinct clustering of 30d samples (Figure 11). To determine the separation of samples more clearly by tissue and time point, PCA was run separately for each treatment group. The AmbT PCA had distinct clusters of each tissue type with a clear developmental gradient of tuber sizes, while the ElevT PCA had merged clusters between tuber stages (Fig. 10). This suggests that ElevT has a differential impact on development and tuber identity compared to AmbT with regards to gene expression.

Differential expression analysis was then completed to determine genes with significant increases or decreases in expression across treatments, tissues and time points using *DESeq2* (Love et al. 2014). In leaves, there were a total of 856 unique differentially expressed genes (DEG) between ElevT and AmbT across all time points, with 305, 383, 120, and 130 DEGs at 30d, 60d, 90d, and 120d comparisons, respectively. To determine general categories of genes that were differentially expressed in these lists, gene ontology (GO) enrichment analysis was completed using *ClusterProfiler* and the TAIR database (Wu et al. 2021; Berardini et al. 2015). In the 60d, 90d, and 120d leaf comparisons, categories related to response to heat, osmotic stress, and abiotic stress were enriched. The 90d and 120d comparisons also had increased expression of GO terms related to polysaccharide, carbohydrate, and sucrose binding and metabolism, as well as several GO terms related to catabolic processes, transport, and localization that showed decreased expression in ElevT. At 30d, most GO terms with decreased expression were related to cellular structures such as chloroplast, plastids, organelles, and cytoplasm, while GO terms

related to macromolecule biosynthesis, response to nitrogen and oxygen-containing compounds, and response to water deficit had increased expression.

When leaf data for all time points were averaged together, 12 genes remained differentially expressed between treatment groups, three with increased expression (Table 3) and nine with decreased expression in ElevT compared to AmbT leaves (Table 4). Genes related to oxidative stress responses had decreased expression in ElevT leaves, including ABA-responsive element binding and peroxidase genes with up to -16.23 log_2-fold change (log_2FC). Additionally, a decrease in a patatin-like gene was seen. Patatin is a storage glycoprotein and makes up about 40% of the total soluble proteins in potato tubers (Weeda et al. 2009). There was also a 14.65 log_2FC increase in a Carboxypeptidase A inhibitor, possibly indicating suppressed degradation and mobilization of proteins in leaves under ElevT. Additionally, a NAC transcription factor gene had increased expression; NAC family proteins are known to play various roles in development and stress responses of plants (Bian et al. 2020).

Gene ID	Log_2FC	*p*-adjusted	Functional Annotation
Soltu.DM.07G016210	14.65	0.011	Carboxypeptidase A inhibitor
Soltu.DM.02G019450	14.32	0.011	terpene synthase
Soltu.DM.07G024710	3.09	1.11E-05	NAC (No Apical Meristem) transcription factor

Table 3. Genes with increased expression in ElevT leaves compared to AmbT leaves. Log_2FC represents the log2 fold-change in ElevT relative to AmbT. The *p*-adjusted value represents the false discovery rate adjusted value using a Bonferroni correction. DEGs were determined using *DESeq2* (Love et al. 2014). Gene IDs correspond to the doubled monoploid (DM) 1-3 516 R44 v6.1 *Solanum tuberosum* genome from SpudDB (http://spuddb.uga.edu).

Gene ID	Log_2FC	*p*-adjusted	Functional Annotation
Soltu.DM.10G030340	-16.23	1.00E-06	ABA-responsive element binding
Soltu.DM.12G002240	-15.66	3.97E-06	Pollen Ole e 1 allergen and extensin
Soltu.DM.08G001570	-15.34	0.008	PATATIN-like
Soltu.DM.05G018810	-14.96	0.034	Peroxidase
Soltu.DM.12G007600	-14.34	0.011	Integrase-type DNA-binding
Soltu.DM.12G025110	-13.10	0.024	conserved hypothetical protein
Soltu.DM.08G004310	-12.88	0.002	IQ-domain
Soltu.DM.03G018250	-3.54	6.43E-12	detoxifying efflux carrier
Soltu.DM.02G024900	-3.25	0.012	dihydroflavonol 4-reductase

Table 4. Genes with decreased expression in ElevT leaves compared to AmbT leaves. Log_2FC represents the log2 fold-change in ElevT relative to AmbT. The *p*-adjusted value represents the false discovery rate adjusted value using a Bonferroni correction. DEGs were determined using *DESeq2* (Love et al. 2014). Gene IDs correspond to the doubled monoploid (DM) 1-3 516 R44 v6.1 *Solanum tuberosum* genome from SpudDB (http://spuddb.uga.edu).

To compare gene expression between tuber developmental stages, expression data for all time points were averaged together per tuber size class and compared across adjacent tuber stages (TI vs. IMT; IMT vs. MAT) under AmbT and ElevT temperatures separately (Figure 12). The aim was to look at which genes change developmentally under normal (AmbT) conditions and find developmental genes that are perturbed by ElevT. I hypothesize that genes that are differentially expressed in both AmbT and ElevT in tubers likely represent core developmental genes, while DEGs exclusive to comparisons under either treatment likely represent temperature-sensitive genes. The functional annotations for DEGs from all comparisons between tuber size classes were largely the same, with many catalytic enzymes, transporters, signaling proteins, transcription factors, and enzymes related to biosynthesis. Presumably, these control the metabolism and transport of resources and the building of cellular components for storage. There

were 1,271 total DEGs between IMTs and MATs under AmbT, compared to 1,095 total DEGs from the same comparison under ElevT. Additionally, there were 4,109 DEGs between TIs and IMTs under AmbT and 3,838 total DEGs under ElevT (Fig. 12). There were 144 shared DEGs between IMT vs. MAT under ElevT comparison and both of the TI vs. IMT comparisons, contrasting with 44 DEGs shared between IMT vs. MAT under AmbT and earlier stages.

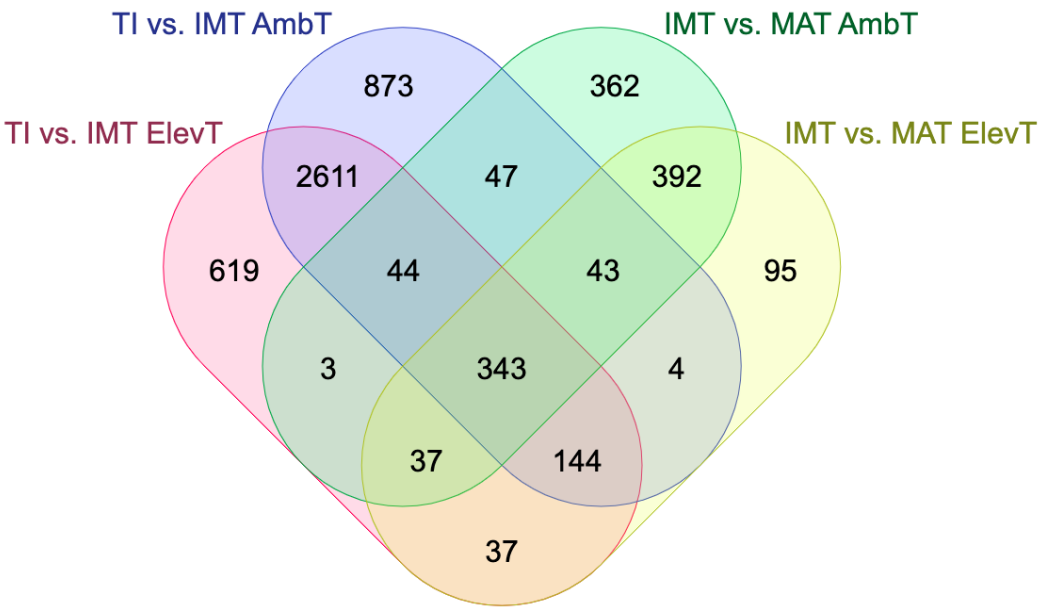

Figure 12. Venn diagram highlighting the number of shared DEGs between developmental stages of tubers under both AmbT and ElevT. DEGs were determined using *DESeq2* (Love et al. 2014). Venn diagram was made using https://molbiotools.com/listcompare.php.

Upon GO enrichment of the TI vs. IMT comparison, both treatment groups had increased expression of GO terms related to starch biosynthesis, helicase activity, RNA splicing/modifications, and ribosomal metabolism in IMTs compared to TIs. Both groups also had decreased expression of GO terms related to oxidoreductase activity, responses to external stimuli, and cell wall/extracellular region in IMTs compared to TIs. Under AmbT, IMTs also had decreased expression of GO terms of responses to endogenous stimuli/hormones compared to

TIs, but these annotations were not present under ElevT. Between IMTs and MATs, comparisons under both AmbT and ElevT had increased expression of GO terms related to RNA processing, ribosomal metabolism, and translation in MATs compared to IMTs, and they also shared categories with decreased expression related to oxidoreductase activity, iron ion binding, monooxygenase activity, and defense response. In addition, the ElevT comparison had GO terms with decreased expression related to metabolism and biosynthesis of secondary metabolites, phenylpropanoid, and wax/fatty acid derivatives, as well as response to stress in MATs compared to IMTs, while these were not present in the AmbT comparison. The AmbT comparison also had GO terms with decreased expression related to biotic stimuli and increased expression in an amide biosynthesis term.

37 DEGs were found to be shared by all tuber development stages exclusively under ElevT, with 13 having increased expression (Table 5) and 24 having decreased expression in larger tuber sizes compared to smaller sizes (Table 6). The DEGs with decreased expression included degradation enzymes such as peptidases, GDSL lipases, and serine carboxypeptidase. There was also a decrease in another NAC domain gene, contrasting with what was seen in leaves. Meanwhile, there were increases in genes related to transcription/translation, such as a SAWADEE domain gene, a TGACG motif-binding factor, and an RNA helicase.

Gene ID	**Log_2FC**	***p*-adjusted**	**Functional Annotation**
Soltu.DM.07G015090	2.84	0.024	SAWADEE domain
Soltu.DM.03G021490	1.17	0.034	Late embryogenesis abundant (LEA) hydroxyproline-rich glycoprotein
Soltu.DM.02G030140	1.01	0.049	Protein of unknown function (DUF1262)
Soltu.DM.01G043220	0.88	0.047	Protein of unknown function (DUF3411)
Soltu.DM.04G028540	0.88	0.027	TGACG motif-binding factor

Soltu.DM.08G024900	0.75	0.003	peroxin 19-2
Soltu.DM.12G016650	0.59	0.003	Protein of unknown function (DUF1421)
Soltu.DM.01G020280	0.45	0.016	NAD(P)-linked oxidoreductase
Soltu.DM.12G004600	0.42	0.041	conserved hypothetical protein
Soltu.DM.06G003370	0.40	0.011	RNA helicase, ATP-dependent, SK12/DOB1 protein

Table 5. Top 10 DEGs with increased expression in larger tuber sizes compared to smaller sizes exclusive to ElevT interactions. Log_2FC represents the log_2 fold-change in ElevT relative to AmbT. The *p*-adjusted value represents the Bonferroni corrected for false discovery rate. DEGs were determined using *DESeq2* (Love et al. 2014). Gene IDs correspond to the doubled monoploid (DM) 1-3 516 R44 v6.1 *Solanum tuberosum* genome from SpudDB (http://spuddb.uga.edu).

Gene ID	**Log_2FC**	***p*-adjusted**	**Functional Annotation**
Soltu.DM.12G007040	-3.44	0.034	peptidase
Soltu.DM.07G028300	-2.88	0.023	NAC domain
Soltu.DM.06G017110	-2.81	0.022	ferulic acid 5-hydroxylase
Soltu.DM.03G008210	-2.77	0.027	cytochrome P450, family 71, subfamily B, polypeptide
Soltu.DM.03G031310	-2.35	0.044	Integrase-type DNA-binding
Soltu.DM.07G026110	-2.26	0.049	conserved hypothetical protein
Soltu.DM.02G015380	-2.16	0.047	conserved hypothetical protein
Soltu.DM.02G019000	-2.07	0.048	FAD-binding Berberine
Soltu.DM.11G026610	-2.07	0.016	Domain of unknown function (DUF966)
Soltu.DM.06G013800	-1.98	0.013	Calcium-binding EF-hand

Table 6. Top 10 DEGs with decreased expression in larger tuber sizes compared to smaller sizes exclusive to ElevT interactions. Log_2FC represents the log_2 fold-change in ElevT relative to AmbT. The *p*-adjusted value represents the Bonferroni corrected for false discovery rate. DEGs were determined using *DESeq2* (Love et al. 2014). Gene IDs correspond to the doubled

monoploid (DM) 1-3 516 R44 v6.1 *Solanum tuberosum* genome from SpudDB (http://spuddb.uga.edu).

Because tuber initiation is a pivotal step in tuberization, I looked at differentially expressed genes in TIs between AmbT and ElevT. In TIs, there were a total of 4,472 unique DEGs between ElevT and AmbT groups from all pairwise time point comparisons. The 120d comparison had by far the most differences with a total of 4,316 DEGs, while there were zero, 91, and 168 DEGs in the 30d, 60d, and 90d comparisons respectively. Upon GO enrichment of these DEGs, 30d, 60d, and 120d time points shared GO terms with increased expression related to cellular component biogenesis and localization (Figure 13). At 60d, most GO terms with increased expression were related to protein-complex assembly and organization as well as response to oxidative stress. Categories with decreased expression at 60d included catabolic processes and organic acid metabolism (Fig. 13a). At 90d, there was an increase in expression of GO terms related to membranes and transmembrane transport, while categories with decreased expression included response to hormone, enzyme inhibitor activity, secretory vesicle/apoplast, and terpenoid biosynthesis (Fig. 13b). At 120d, enrichment of the 4,316 DEGs revealed increased expression of GO terms related to the cell cycle, cell wall, and the extracellular region, while categories with decreased expression were related to response to ethylene and salicylic acid, response to hypoxia, mRNA regulation, and one floral organ senescence term (Fig. 13c). Additionally, 17 auxin-related DEGs were found in the list of 4,316 DEGs at 120d, as well as four gibberellin-regulated DEGs with increased expression and four GA-oxidase DEGs, three of which had decreased expression.

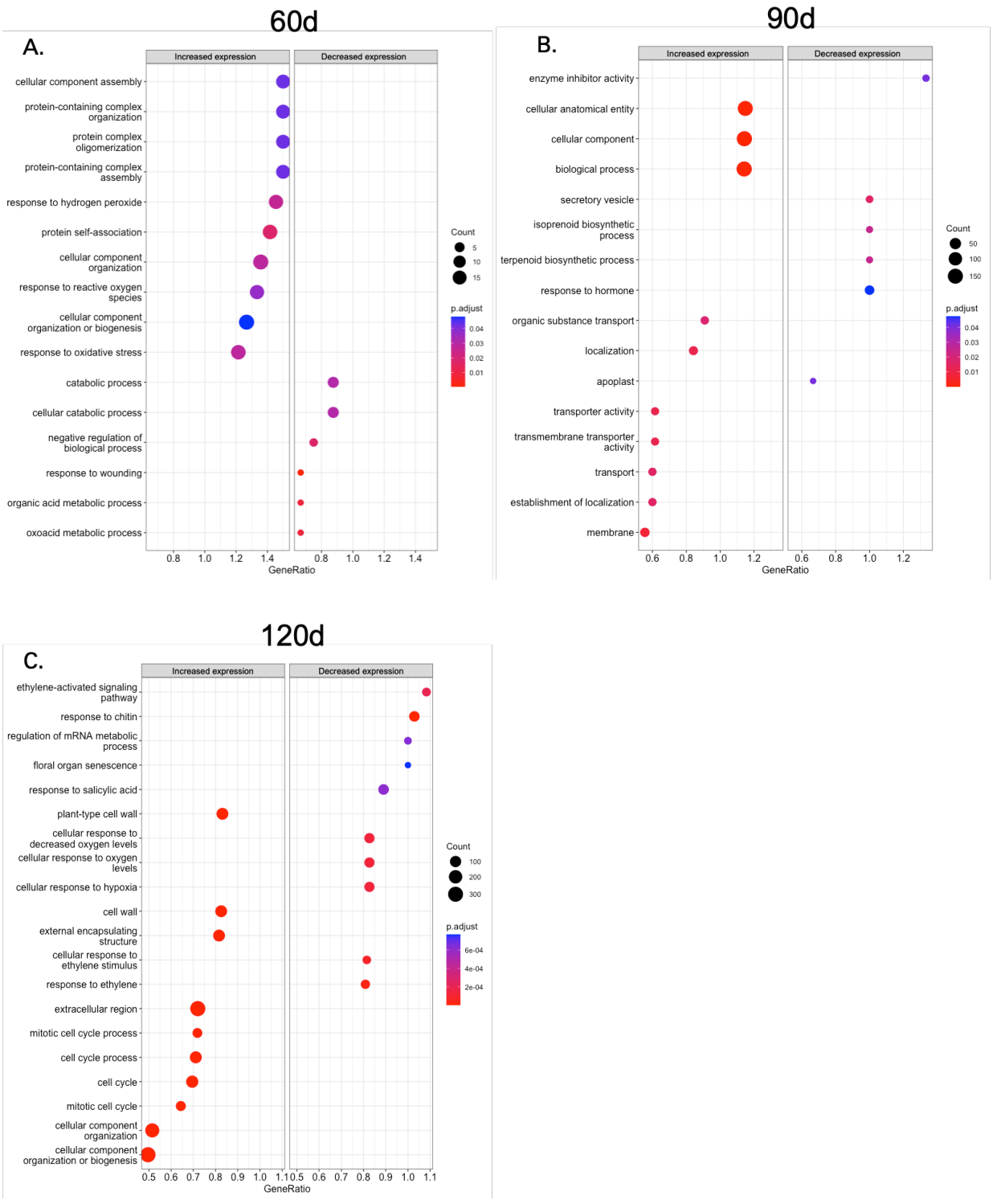

Figure 13. GO enrichment of 60d (A), 90d (B), and 120d (C) DEGs from ElevT vs. AmbT comparisons in tuber initials (TIs). Dot plots were made using *ClusterProfiler* in R and the TAIR database (Wu et al. 2021; Berardini et al. 2015).

To see how ElevT affects tubers in later stages of development, differentially expressed genes in IMTs and MATs between ElevT and AmbT were explored. No IMTs or MATs were collected at 30d, so comparisons were made for later time points only. At 60d, there were 129 DEGs in IMTs between ElevT and AmbT. Differential gene expression analysis could not be completed for IMTs at other time points because not enough biological replicates were collected. GO enrichment of the 129 DEGs revealed increased expression of GO terms related to response to stress, temperature/heat, oxidative stress, and protein folding. GO terms with decreased expression included categories related to response to lipid/fatty acids and organic compound metabolism. The list of 129 DEGs in IMTs also included 11 kinase/receptor related DEGs, nine of which had decreased expression, as well as 18 heat shock related genes and 16 histone related genes which all had increased expression.

In MATs, there were 520 total unique DEGs between ElevT and AmbT, with 46 DEGs at 60d and 478 DEGs at 120d. No MATs were collected from ElevT plants at 90d, so differential expression analysis could not be completed for that time point. GO enrichment of the 478 DEGs at 120d revealed increased expression of categories related to cell cycle and cellular components, while categories with decreased expression were mostly related to decreased oxygen levels. The top 10 DEGs between ElevT and AmbT MATs at 120d included two lipid transfer genes and a pectin lyase-like gene with increased expression, and two kunitz trypsin inhibitors and a SAUR-like auxin-responsive gene with decreased expression (Table 7). The list of 478 DEGs in MATs at 120d also included five other kunitz family proteinase inhibitors, four of which had decreased expression. Three other proteinase inhibitors, including a kunitz family, potato type I and potato type II proteinase inhibitors also had decreased expression in MATs under ElevT at 60d. Additionally, 10 proteases and 11 histone genes were found in the list of 478 DEGs to have

increased expression in MATs under ElevT, along with one histone deacetylase gene which had decreased expression. 23 kinase/receptor-related genes and four heat shock genes were also found to be differentially expressed in this list.

Gene ID	Log_2FC	*p*-adjusted	Functional Annotation
Soltu.DM.12G010360	4.92	1.61E-18	delta tonoplast integral protein
Soltu.DM.07G019090	-3.35	2.35E-18	Wound-responsive family protein
Soltu.DM.01G021910	4.53	2.62E-18	Bifunctional inhibitor/lipid-transfer /seed storage 2S albumin
Soltu.DM.04G036370	-2.87	1.63E-15	SAUR-like auxin-responsive
Soltu.DM.03G018570	-1.94	4.78E-15	kunitz trypsin inhibitor
Soltu.DM.03G018670	-2.34	5.56E-15	kunitz trypsin inhibitor
Soltu.DM.05G009050	2.17	2.56E-13	Pectin lyase-like
Soltu.DM.06G017220	2.85	9.63E-12	cytochrome P450, family 71, subfamily B, polypeptide
Soltu.DM.02G030450	3.46	1.02E-11	GAST1 homolog
Soltu.DM.08G025250	4.90	1.36E-11	Bifunctional inhibitor/lipid-transfer /seed storage 2S albumin

Table 7. Top 10 DEGs in MATs between ElevT and AmbT at 120d. Log_2FC represents the log_2 fold-change in ElevT relative to AmbT. The *p*-adjusted value represents the Bonferroni corrected for false discovery rate. DEGs were determined using *DESeq2* (Love et al. 2014). Gene IDs correspond to the doubled monoploid (DM) 1-3 516 R44 v6.1 *Solanum tuberosum* genome from SpudDB (http://spuddb.uga.edu).

Expression Patterns of Known Regulators in Tuberization Signaling

I then investigated the gene expression patterns of key genes and known regulators involved in tuberization signaling in potato, starting with SP6A (Soltu.DM.05G026370), the known tuberigen which is produced mainly in leaves as a mobile signal (Navarro et al. 2011). SP6A

expression in leaves was consistent with its known expression pattern, starting out low (0.1 TPM) in early stages and accumulating over time (98.9 TPM) (Figure 14; Park et al. 2022). SP6A expression in leaves under ElevT was slightly lower than that of AmbT (-1.1 log_2FC), consistent with previous work, but was not found to be differentially expressed in our experiment ($p > 0.05$) (Park et al. 2022). BEL5 (Soltu.DM.06G029500), a transcriptional promoter of SP6A and other genes involved in tuberization that is expressed in many tissues, had similar expression patterns to SP6A with expression being slightly decreased in ElevT leaves (-0.6 log_2FC; $p > 0.05$) (Sharma et al. 2016). In TIs, BEL5 showed slightly (0.13 log_2FC) increased expression in ElevT compared to AmbT but was not differentially expressed ($p < 0.05$) (Fig. 14). In IMTs, BEL5 had increased expression at 120d, although statistical analyses between treatments were not able to be completed for IMTs at 90 and 120d as there were not enough biological replicates. There were no significant differences in expression of BEL5 in MATs between ElevT and AmbT.

IT1 (Soltu.DM.06G025210) is a gene that was recently found to be responsible for the differentiation of stolons into tubers (Tang et al. 2022). In AmbT, IT1 expression was highest in TIs and starts out high at 44.4 TPM at 30d, then drops by 57% throughout the rest of the growing period. This expression pattern was the same but slightly lower with up to 2.7 log_2FC decrease in TIs under ElevT (Fig. 14). This pattern may be because all TIs collected at 30d were in very early stages of development before the stolons had begun to swell (Supplementary Figure 3). At subsequent time points, however, TIs in later stages of development were collected and pooled together. It is possible that IT1 is highly expressed only in very early stages of TIs before the stolon has begun to swell, and pooling of TIs even in subsequent stages of development may have diluted the expression of IT1 in our later data. Interestingly, ElevT IMTs and MATs had

opposite expression patterns of IT1 than in AmbT tubers, with expression increasing over time. The importance of IT1 expression in growing tubers is unknown as it has only recently been discovered, although its role seems to be most pivotal in stolons. Because of this, I also would not expect this gene to be expressed in leaves, which is confirmed by very low expression in our data (< 1.5 TPM).

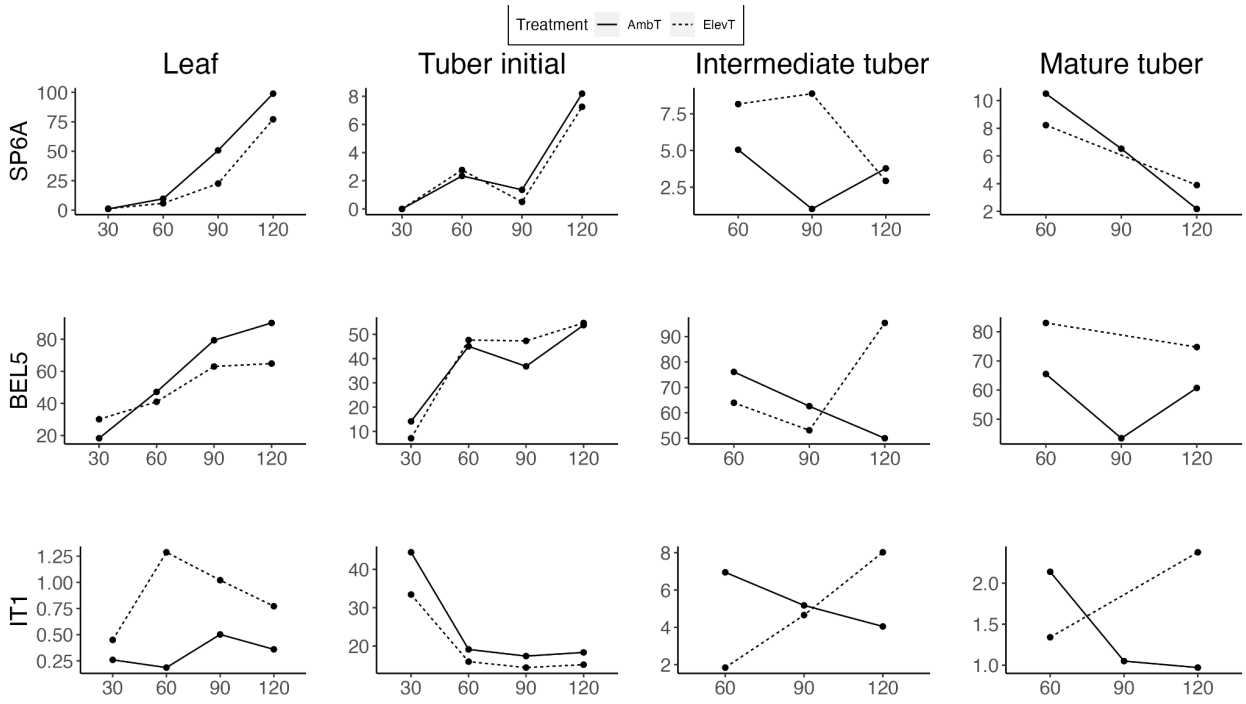

Figure 14. TPMs of known tuberization promoter genes (SP6A - Top Row, BEL5 - Middle Row, and IT1 - Bottom Row) in each tissue type over the course of 120 days. No ElevT mature tubers were collected at 90d, so no data is shown for that point. TPM values were determined from *Salmon* (Patro et al. 2017) and averaged per biological replicate (n = 1 or 2).

TOC1 (Soltu.DM.06G025760) is a core circadian clock gene and known temperature-sensitive inhibitor of SP6A expressed in both leaves and tubers, and previous work has shown increased expression levels of TOC1 in developing tubers under moderately ElevT (Morris et al. 2019; Hancock et al. 2014). In this experiment, TOC1 had significantly decreased expression (p < 0.05) in IMTs and MATs compared to TIs under AmbT, indicating that a decrease in TOC1

expression in developing tubers may be involved in growth (Figure 15). However, TOC1 was not differentially expressed in IMTs compared to TIs under ElevT. This suggests that TOC1 may not decrease in developing tubers under elevated temperature, possibly contributing to suppression of SP6A and/or tuber growth. TOC1 also had up to -1.2 log_2FC decrease in expression in leaves under ElevT at 60 and 90d but was not differentially expressed ($p > 0.05$). Its expression pattern in TIs was largely similar under both treatments with a 66% increase from 30d to 120d in both treatments, and there was slight (0.5 log_2FC) increased expression in ElevT compared to AmbT at 90d ($p > 0.05$) (Fig. 15).

The COL1-SP5G inhibitory pathway is known to be an important suppressor of tuberization under long-day photoperiods (Abelenda et al. 2016). Both genes are known to act primarily in leaves, although expression of both has also been found in tubers (Abelenda et al. 2016; Park et al. 2022). There are two SP5G-like genes, SP5G-A and SP5G-B (Zhang et al. 2021a), but SP5G-A (Soltu.DM.05G024030) is the primary inhibitor associated with COL1 (Soltu.DM.02G030260) in previous studies (Abelenda et al. 2016). In this experiment, both COL1 and SP5G-A had up to 1.8 log_2FC increased expression in leaves at most collection days ($p > 0.05$), although SP5G-A had a significant -4 log_2FC decrease in ElevT leaves at 60d only ($p < 0.02$) (Fig. 15). COL1 expression was increased under ElevT in TIs by up to 1.3 log_2FC increase, although it was not found to be differentially expressed ($p > 0.05$) (Fig. 11). Additionally, COL1 was significantly decreased by -1.67 log_2FC in ElevT IMTs at 60d ($p < 0.009$). No significant differences in COL1 expression were found between treatments in MATs. SP5G-A had lower expression in ElevT TIs at most time points, consistent with findings in similar experiments (Park et al. 2022) but had significantly increased levels at 120d (2.56 log_2FC; $p < 0.043$). SP5G-A was also significantly decreased in MATs under ElevT by -1

log_2FC ($p < 0.02$). This data suggests the COL1-SP5G inhibitory pathway is possibly temperature-sensitive, although there may be other thermo-regulatory genes/mechanisms responsible for tuber inhibition under heat stress.

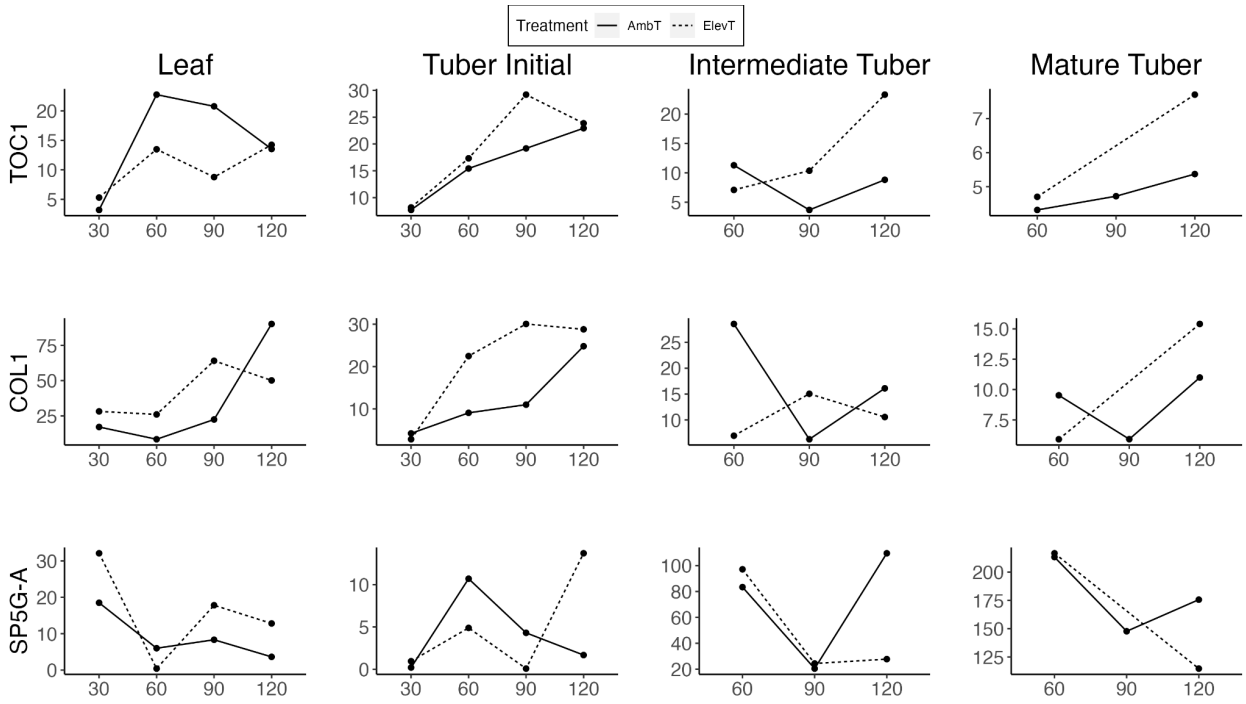

Figure 15. TPM expressions of known tuberization inhibitor genes (TOC1 - Top Row, COL1 - Middle Row, and SP5G-A - Bottom Row) in each tissue type collected over 120 days. No ElevT mature tubers were collected at 90d, so no data is shown for that point. TPM values were determined from *Salmon* (Patro et al. 2017) and averaged per biological replicate (n = 1 or 2).

Many of the crucial tuberization signaling genes are part of the PEBP family, notably SP6A, but also StCEN, SP5G, and other flowering related genes that have recently been found to contribute to tuberization such as StSP3D and StFTL1 (Zhang et al. 2020; Jing et al. 2023). Some of these genes are in the FT subfamily, such as SP6A and SP3D, while others are in the TFL subfamily, such as CEN (Supplementary Table 3; Zhang et al. 2022). One gene, StPEBP6, is in the MFT subfamily. Because our data does not suggest photoassimilate production as a cause for yield loss, and a reduction in sink strength caused by internal signals is more likely, I

decided to look at expression of all 15 PEBP family members (Figure 16). Gene IDs for all PEBP genes are shown in Supplementary Table 3. Here, I saw somewhat clear patterns showing which PEBP genes are expressed in leaves, TIs, IMTs, and MATs over time in both treatment groups. This pattern is less clear in tubers under ElevT, with genes such as StPEBP1, StPEBP12, and StPEBP2 having different expression patterns than under AmbT. Additionally, a gene that has not been well studied called StPEBP6 (Soltu.DM.03G033490) had significantly increased expression in IMTs compared to TIs under ElevT ($p < 0.05$), but this gene was not differentially expressed in the AmbT comparison. It also appeared that most genes in the FT subfamily, specifically SP6A, SP3D, and FTL1, tend to have decreased expression in ElevT leaves compared to control, while genes in the TFL subfamily tend to have increased expression in tissues under ElevT, especially StSP9D, StPEBP10, and StPEBP1. Not all genes follow this pattern, however, and none of these mentioned genes were found to be differentially expressed between ElevT and AmbT ($p > 0.05$). Both inhibitors SP5G-A and SP5G-B were differentially expressed between tuber size classes under AmbT, but only SP5G-A was found to be differentially expressed in different tuber sizes under ElevT ($p < 0.05$). Both SP5G-A and SP5G-B had significantly increased expression in ElevT TIs compared to AmbT at 120d (2.6 and 8.7 $\log_2$FC, respectively; $p < 0.05$). Additionally, CEN, a known inhibitor of the tuberigen activation complex (TAC), was found to be slightly decreased in ElevT TIs at 120d (-1.28 $\log_2$FC), although it was not differentially expressed ($p > 0.05$). These differences in expression call for more future research on unstudied PEBP genes and their effects on tuberization under elevated temperatures.

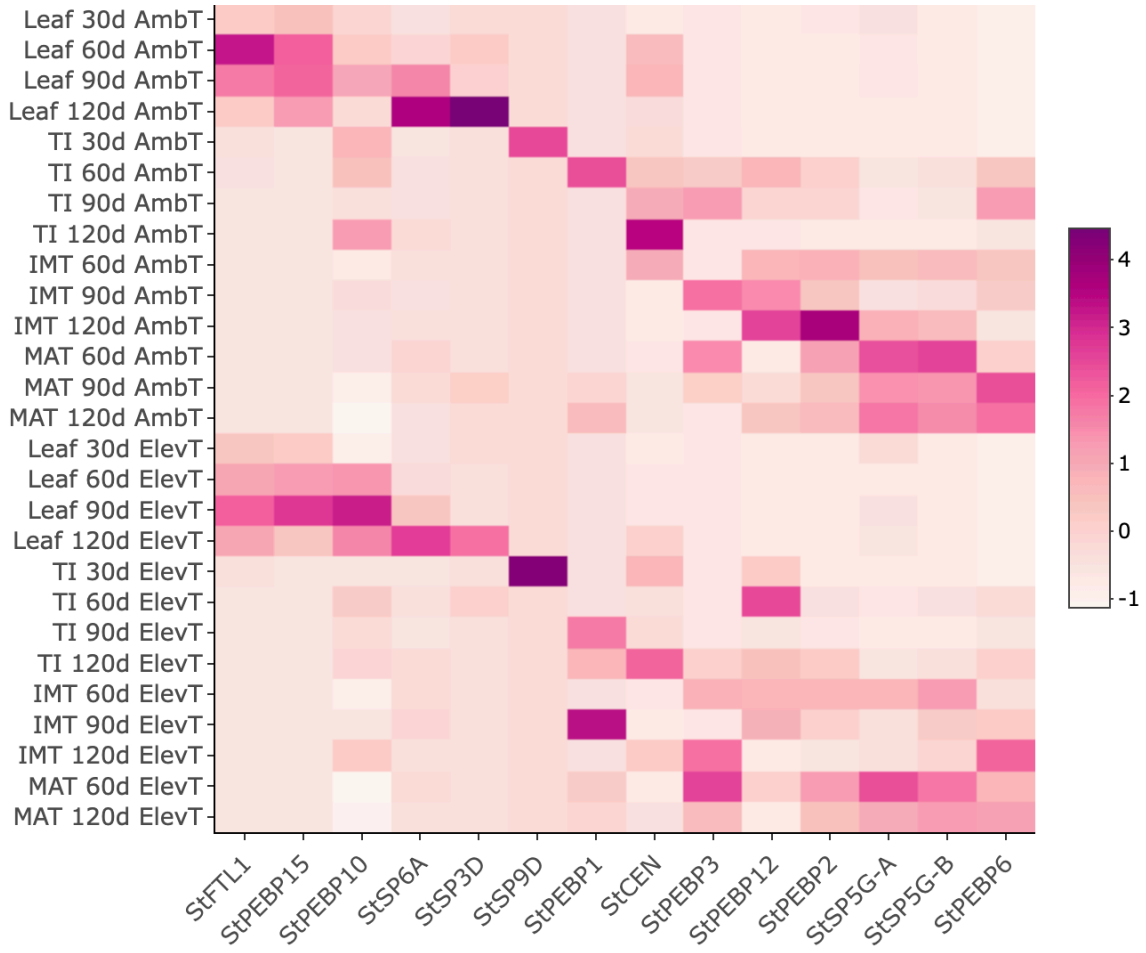

Figure 16. Gene expression heatmap of all PEBP family genes in each tissue over all collection days, separated by treatment (AmbT on top, ElevT below). Many of these PEBP genes have not been thoroughly studied, so the ones without set gene names in literature are referred to as StPEBP(1-15) as named in Zhang et al. (2022). StPEBP13 had zero expression for all libraries and was not included in the heatmap. Values are TPM expressions averaged per biological replicate (n = 1 or 2) and scaled to z-scores by column. Figure was made using *heatmaply* package in R (https://github.com/talgalili/heatmaply).

Coexpression Analysis

To find gene networks that are involved in tuberization and possibly temperature-sensitive pathways, I used $\log_{10}$-transformed TPM values from *Salmon* as input for a gene coexpression analysis using the Simple Tidy workflow (Patro et al. 2017; Li and Buell 2022). Overall, 26 modules with at least 5 genes were produced with all tissue types and treatment groups run

together in the analysis (Figure 17). Of these, modules 2, 10, and 23 were of interest due to their coexpression patterns and location of known genes involved in tuberization signaling. SP5G-A and SP5G-B were found in Module 10, which contained 722 total genes and shared exactly 315 genes with AmbT and 315 with ElevT tuber development DEGs, although these genes were not all mutual between treatments. This module had the highest expression in TIs and contained functional annotations related to tuberization, such as proteases, carboxypeptidases, patatin-like genes, and proteinase inhibitors. Module 2 had the highest expression in TIs and contained 1003 total genes, 350 of which were shared with AmbT DEGs between tuber size classes, and 319 of which were shared with ElevT tuber size class DEGs. These shared DEGs in Module 2 had functions mostly related to tuberization, similar to Module 2. Module 23 had the highest expression in TIs and contained 133 total genes, 53 of which had heat shock related functional annotations. 74 of these genes were found in the lists of DEGs in TIs, 15 were shared with DEGs in IMTs, and 10 were found in the lists of DEGs in MATs between ElevT and AmbT.

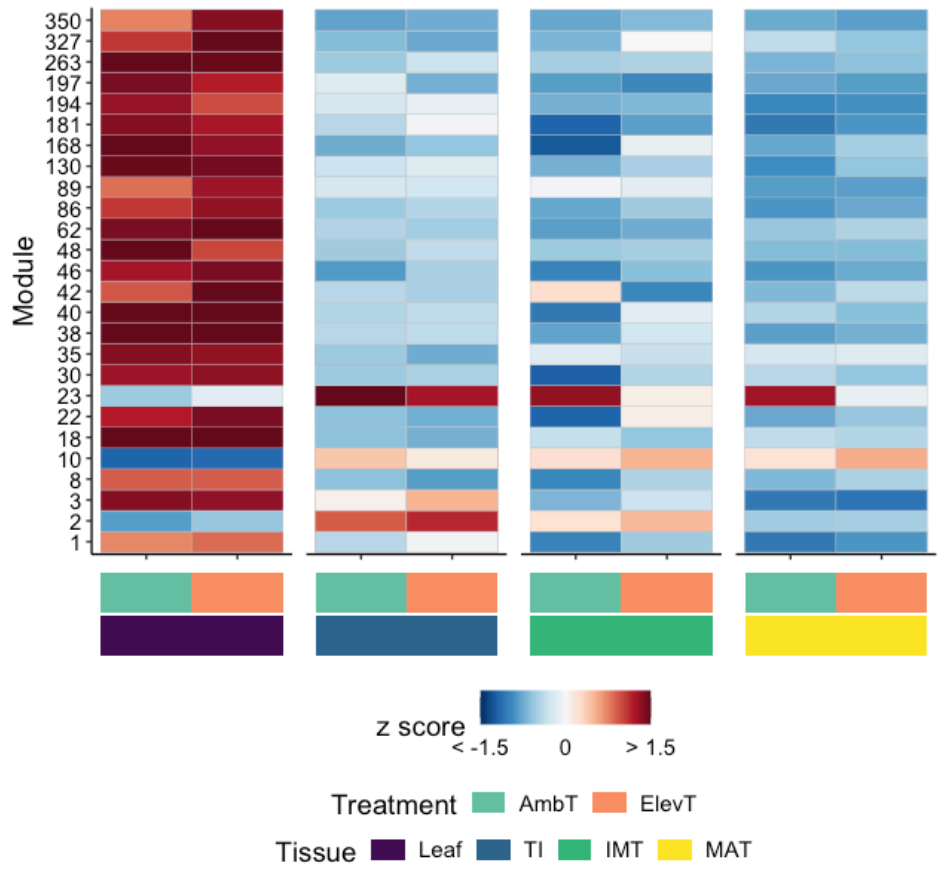

Figure 17. Heat map of clustered gene z-scores per tissue and treatment for each module. Produced using the Simple Tidy gene coexpression analysis workflow (Li & Buell 2022).

Discussion

Photosynthetic Parameters Cannot Explain Yield Loss Under Heat Stress

In this study, I investigated the mechanisms of yield loss that is displayed when potato plants are exposed to higher-than-optimum temperatures. I measured aspects of leaf physiology and found that carbon assimilation, stomatal conductance, and rate of leaf senescence of ElevT plants were consistent with the control group at every time point other than 60d (Figs. 3 & 4). Upon experiencing water deficit, plants produce signals to close their stomatal pores, thus reducing

transpiration and conserving water. This action significantly reduces gas exchange of leaves (Galmés et al. 2013). Since I observed the ElevT plants to have visibly drier soil than the AmbT plants at 60d, the significantly lowered rates of carbon assimilation and stomatal conductance at that time point are most likely due to insufficient watering. One study reported higher rates of transpiration in one cultivar of potato plants grown under higher temperatures, which supports our hypothesis of increased evapotranspiration contributing to the dry soil of ElevT plants at 60d (Singh et al. 2015). Additionally, leaf senescence rates were largely consistent between treatment groups except at 60d, when measurements of photosystem II efficiency in ElevT leaves remained higher than AmbT leaves after 72hr of dark-induced senescence (Fig. 4). Although this slowed rate of leaf senescence is contrary to general knowledge about drought responses in plants inducing leaf senescence (Jan et al. 2019), the fact that measurements of photosystem II were consistent between AmbT and ElevT at every other time point indicate that this effect is likely related to the water deficit conditions observed at 60d. Despite these observed effects, our results suggest that chronic elevated temperature does not significantly impact the photosynthesis or senescence of potato plants when water availability is not a concern. In fact, some later time points in this study showed slightly higher rates of gas exchange under ElevT (Fig. 3). These results are concurrent with other studies that found no significant or positive effects of high temperatures on photosynthetic rates in potato (Park et al. 2022; Hancock et al. 2014). Furthermore, chlorophyll content of leaves was unchanged between AmbT and ElevT treatments in this study, consistent with previous findings of no significant effects of higher temperatures on total leaf chlorophyll levels (Singh et al. 2015). However unintended, the observed effect of drier soil in ElevT plants highlights the frequent co-occurrence of heat and drought stress, especially since less precipitation is often seen in some regions experiencing increases in temperatures

(IPCC, 2021). This could be a possible reason for reports of decreased photosynthesis of potato plants in other studies that may not have taken differences in water use into account.

Potato tubers are storage organs of the plant, formed from the transport and deposition of sucrose and other photoassimilates from the leaves to stolon tips (Zierer et al. 2021). One hypothesis in early literature for the observed yield loss of potato plants under heat stress is a reduction of photoassimilate production in the leaves, causing reduced source-sink transport (Wolf et al. 1990). Carbohydrate analyses of leaves in other studies report an accumulation of sugars such as sucrose, glucose, and fructose in potato leaves under heat stress (Park et al 2022). Additionally, many studies report significant increases in aboveground biomass of potato plants exposed to high temperatures (Tang et al. 2018; Park et al. 2022; Timlin et al. 2006). Although there were no significant differences in aboveground biomass observed in this study, measurements increased slightly under ElevT (Fig. 7), consistent with findings in literature. Furthermore, differential gene expression analysis of leaf tissue in our experiment revealed increased expression of GO terms related to polysaccharide/carbohydrate and sucrose binding and metabolism in ElevT leaves, as well as decreased expression of GO terms related to catabolic processes and transport. These results suggest that carbohydrates and other resources are stored in the leaves of ElevT plants more so than in AmbT plants, and that there is a reduction in the catabolism and mobilization of resources out of leaves under ElevT. Thus, a reduction in photoassimilate production is not a likely driver of yield loss under heat stress. Instead, regulation of resource transport through molecular signaling is a possible driver behind tuber inhibition under heat stress, resulting in a shift in biomass allocation towards the aboveground plant and suppressing starch accumulation in tubers.

Chronic Elevated Temperatures Inhibit Tuber Filling, But Not Initiation

Tuber production of a potato plant consists of two separate processes: tuber formation/initiation and tuber filling. In this study, TIs and IMTs were still observed under ElevT, with no significant change from AmbT numbers (Fig. 5; Table 1). Other studies report a delay in tuberization in potato plants experiencing heat stress (Park et al. 2022; Van Dam et al. 1996). In this study, I observed a slight delay in tuberization in ElevT plants as there were slightly less TIs collected under ElevT at 60d compared to AmbT; however, at later time points, the number of TIs collected from AmbT and ElevT were largely similar, with even slightly more TIs collected from ElevT plants at 120d (Fig. 5). Despite this, I still observed a significant decrease in MATs collected from ElevT plants. Additionally, some significant changes in hormone levels were seen particularly in ElevT IMTs. ABA active forms had the largest decrease in IMTs under ElevT compared to other tissues, and the highest increases in phenolic compounds such as sinapic and benzoic acid were seen in IMTs collected from ElevT plants compared to AmbT plants, possibly contributing to the inhibited filling of initiated tubers (Fig. 9). These results indicate that tuber initiation is not significantly inhibited under chronic elevated temperatures, but that some interference in developing tubers under ElevT prevents them from filling to maturity.

Taken together, the results from this study support the idea that potato plants under heat stress still attempt to produce tubers, but mis-signaling occurs between tuber initiation and maturation, inhibiting their continued growth. The exact fate of tubers that do not make it to maturity is still unclear. Until recently, it has generally been understood that tuber development is continuous, and that final tuber size is determined by genetics and the environmental factors experienced during development. However, a recent study (Jia et al. 2022) has shown that even under normal temperatures, not all initiated tubers make it to maturity, and some initiated tubers

disappear before harvest and degrade during the growing period. Differential gene expression analysis revealed the upregulation of carbohydrate metabolism and sucrose transport genes in degrading tubers, likely attributing the degradation process to a competition for carbohydrates. Considering a shift in carbohydrate metabolism is seen in potato plants grown under elevated temperatures (Timlin et al. 2006), it is possible a similar degradation mechanism plays a role in yield loss under heat stress. Additionally, many protease inhibitor genes were downregulated in degrading tubers in the study. Proteinase inhibitors, such as ones in the kunitz family, potato type I, and type II-type proteinase inhibitors, are crucial for the accumulation of storage proteins in tubers and for keeping them in dormancy as they prevent the catabolism of storage structures (Weeda et al. 2009). The results from the Jia et al. (2022) study support the idea that resources in degrading tubers are broken down and remobilized to the above ground plant. In this experiment, I did not observe many differentially expressed genes related to carbohydrate/sucrose transport in tubers between treatment groups, indicating that tubers under ElevT may not be actively reallocating resources back to the aboveground plant. However, I did see decreased expression of several differentially expressed proteinase inhibitors including kunitz family and potato type I and type II proteinase inhibitors, as well as increases in several aspartyl proteases, particularly in MATs under ElevT (Table 6). These results suggest that mechanisms to keep resources stored within tubers may not properly occur under ElevT, such as the expression of proteinase inhibitors. This could also potentially explain the reports of heat sprouts and early dormancy breaks seen in potatoes grown under high temperatures (Zhang et al. 2021b). In future studies, it would be interesting to record the number of degraded tubers under elevated temperatures and see if there is an increase in number compared to growth under normal temperatures, as well as look for signaling molecules that may initiate this degradation process.

In this study, I grouped all stolons with a mass less than 0.6g into one developmental class. However, the transition of a stolon to tuber is a very nuanced process that is still not completely understood, especially under the context of elevated temperature. In future studies, it may be enlightening to collect and classify stolons into more specific stages of development, such as the stages described in Weeda et al. (2007).

Changes In Internal Signaling May Impact Sink Strength Under Heat Stress

Internal signaling in potato plants is crucial for the formation and maintenance of sink strength of tubers, both through genetic regulation and through production of hormones. In the present study, I found significant changes in endogenous phytohormone levels in potato plants under ElevT vs. AmbT. Total auxin levels were reduced in ElevT leaves compared to AmbT leaves, particularly in levels of OxIAA along with slightly lower levels of most auxin metabolites (Fig. 8; Table 2). OxIAA is a primary catabolite of IAA; the catabolism of IAA to OxIAA is an irreversible process that dramatically reduces the activity level of the molecule (Pencík et al. 2013). However, there were higher levels of OxIAA-GE, a glucose ester conjugated form of OxIAA, in the larger tuber sizes of ElevT compared to AmbT. Changes in levels of inactivated forms of hormones could indicate changes in overall levels of the active forms (Pencík et al. 2013). In addition, several auxin responsive DEGs were found in comparisons between AmbT and ElevT in both leaves and tubers (Table 7). These results suggest a role of auxin signaling in tuberization under elevated temperatures.

Remarkably, levels of basal ABA were significantly reduced across all tissue types under ElevT, although ABA is typically found to be increased in plants experiencing stress, triggering downstream responses to help the plant cope to an adverse environment (Fig. 9) (Li et al. 2021).

Besides its role in stress response, ABA contributes to aspects of development in *S. tuberosum* through acting antagonistically to GA (Xu et al. 1998; Chen et al. 2022). GA is an important inhibitor of tuberization through inducing stolon elongation rather than radial growth of tubers, and higher GA:ABA ratios in potato plants increase aboveground biomass and inhibit tuber growth (Xu et al. 1998). These results of decreased ABA under ElevT suggest the possibility of higher GA:ABA ratios in ElevT plants, contributing to tuber inhibition. Although GA levels were below detectable levels in the phytohormone analysis of tissues, I did find increased expression of several GA-regulated DEGs in comparisons between ElevT and AmbT tissues, as well as decreased expression of a few GA-oxidase DEGs, particularly in TIs. Additionally, ABA is known to regulate dormancy of potato tubers, with lower levels generally associated with shorter dormancy periods (Wang et al. 2020). This supports our earlier hypothesis of ElevT impacting mechanisms of tuber dormancy through decreased expression of proteinase inhibitors. Although the exact mechanism of how decreased ABA levels contribute to tuber inhibition is unclear, these results indicate that ABA signaling possibly contributes to suppressed tuber development under higher temperatures.

Additionally, some phenolic compounds were increased in tubers under ElevT, especially sinapic and benzoic acid (Table 2). In gene expression comparisons between TIs from AmbT and ElevT plants, I saw decreases in enriched GO terms related to response salicylic acid and ethylene (Fig. 13c). These observed changes in phytohormone levels possibly contribute to the reduction in sink strength and thus reduced yield/the shift in biomass allocation away from the storage organs. This hypothesis is supported by enriched GO terms related to hormone responses in comparisons between tuber size classes under AmbT, whereas these GO terms were not enriched in ElevT comparisons.

In the differential gene expression analysis, many core developmental genes for tuberization were observed between tuber sizes under both treatments, such as catabolic enzymes, carbohydrate metabolism genes, auxin-responsive genes, signaling genes such as kinase and receptor-related genes, and protease inhibitors, which the coexpression analysis revealed many to be part of several gene coexpression clusters (Table 6). ElevT comparisons between tuber size classes yielded less overall DEGs than under AmbT, suggesting that some genes required for growth to maturity may not be expressed under ElevT (Fig. 12). Additionally, the observable difference in clustering of tuber RNA-seq libraries under AmbT and ElevT indicate significant impacts of increased temperatures on gene expression in tubers (Fig. 10).

In the lists of DEGs in tubers between treatments, I observed many kinase/receptor related genes with decreased expression under ElevT, as well as DEGs related to protease activity. Kinases are important enzymes that facilitate signal transduction through phosphorylation of structures (Umezawa et al. 2013). A 2019 study found that the mobilization of important storage proteins in potato, such as patatin, is dictated by their phosphorylation status (Bernal et al. 2019). This study found that proteases preferentially degrade patatin proteins that are highly phosphorylated. Our observation of kinase and protease-related DEGs under ElevT suggests that increased temperatures may affect the mobilization of storage proteins in tubers. Additionally, studies in Arabidopsis have shown links between ABA signaling and ABA-responsive phosphorylation of storage proteins in seeds (Ghelis et al. 2008; Umezawa et al. 2013). Although tubers are not true reproductive seeds, it is possible that similar mechanisms control dormancy breaks in both seeds and potato tubers. Considering the significant decrease in ABA levels observed in ElevT tissues in conjunction with kinase and protease-related DEGs, our results suggest impacts of ElevT on signaling within potato plants that potentially affect storage

protein mobilization. Concurrent with these results, a transcriptomic study on drought stress in potato found decreased expression of both ABA-related and patatin genes, indicating changes in regulation of storage proteins under drought (Da Ros et al. 2020). This suggests the possibility of a similar mechanism of tuber suppression under heat and drought stress, as decreased yields are often seen in potato plants under water deficit (Da Ros et al. 2020). The decrease in gene expression of kinases may also suggest changes in signal transduction of other molecular pathways within tubers under ElevT. Overall, our results suggest changes in signaling within potato plants under ElevT that lead to changes in gene expression in tubers, ultimately affecting regulation of resource transport.

Potential Temperature Sensitive Regulators of Tuberization

There has been considerable work in recent years on understanding the effects of elevated temperature on SP6A expression and its role in tuberization. A previous study observing transgenic SP6A over-expressor lines concluded that SP6A likely controls tuber formation, but not continued growth of tubers as yield was still significantly decreased in transgenic SP6A over-expressor lines under high temperatures (Park et al. 2022). In this study, I saw a slight decrease in SP6A expression in ElevT plants that was not considered differentially expressed, which is consistent with the slight delay in tuberization observed at 60d (Figs. 11 & 5). However, these relatively small differences cannot explain the significant decrease in MATs formed under ElevT. Overall, these results support the hypothesis that SP6A regulates tuber initiation, but that there are other players responsible for the continued growth of tubers. It is also possible that SP6A is inhibited post-translationally under ElevT (Zhang et al. 2020), and there may be other genes inhibiting the SP6A protein or interfering with the formation or function of the

tuberization activation complex (TAC). This hypothesis could explain the significant decrease in MATs collected from ElevT tubers despite only a slight decrease in SP6A transcript expression. In this case, it would be beneficial to study genes that are known to target TAC, such as CEN, a protein that was found to inhibit TAC through competitive binding with the FD-like proteins that are needed for formation of the protein complex (Zhang et al. 2020). Furthermore, CEN overexpressor lines grown under normal temperatures were found to have decreased tuber yield and increased aboveground plant biomass, parallel with the effects seen in potato plants grown under ElevT (Zhang et al. 2020). Although CEN expression was not found to be increased in our study (Fig. 16), more in-depth research on this gene in the context of temperature may be worth exploring.

TOC1 is a known transcriptional inhibitor of tuberization through suppressing promoter activity of SP6A. From our RNA-seq data, I found expression of TOC1 to increase over time in both IMTs and MATs under ElevT (Fig. 15). Additionally, DEG analysis between tuber size classes suggest that TOC1 is most highly expressed in smaller tuber sizes and declines over time under normal development, but that TOC1 expression remains higher in larger tuber sizes under ElevT than under AmbT. This data is consistent with previous studies that have found increases in expression of this gene in tubers under higher temperatures (Hancock et al. 2014; Morris et al. 2019). Functional studies of this gene reveal significant impacts on growth and resource partitioning of potato plants (Morris et al. 2019). Antisense lines of TOC1 in *S. tuberosum* revealed higher expression of SP6A in developing stolons, taller plant height, and significantly higher yield under increased temperatures, compared to wild-type (WT) plants grown under the same conditions (Morris et al. 2019). Parallel to these results, over-expressor lines of TOC1 revealed significantly reduced yield, shorter plant height, and lower SP6A expression in leaves

compared to WT (Morris et al. 2019). Additionally, global gene expression analysis of developing stolons from TOC1 missense lines reveal increases in expression of starch metabolism and heat shock factors compared to WT, indicating that TOC1 is important for inhibiting tuberization and suppressing stress responses under higher temperatures (Morris et al. 2019). Furthermore, studies of the TOC1 homolog in Arabidopsis reveal interactions between TOC1 and ABA-related genes in plants under drought stress (Legnaioli et al. 2009). These results further support our hypothesis of ABA controlling tuberization under ElevT and highlight TOC1 as a potential gene for studying heat tolerance in potato plants.

Recently, two florigens from the PEBP family, SELF PRUNING 3D (StSP3D) and FLOWERING LOCUS T-like 1 (StFTL1), that were long associated exclusively with flowering have been found to be important players in tuberization through secondary activation of SP6A (Jing et al. 2023). Furthermore, grafting experiments with non-tuber forming species (*S. etuberosum)* show that even in the absence of SP6A, SP3D and FTL1 are sufficient signals to induce tuberization in *S. tuberosum* rootstocks (Jing et al. 2023). In our experiment, both of these genes had slightly decreased expression in leaves under ElevT compared to AmbT (Fig. 16). Considering tuberization signaling is similar to the flowering pathway as tubers are a form of modified stem, it could benefit breeding efforts to further study these flowering and related PEBP genes and their roles in tuberization, as the changes in expression patterns of these genes seen in this study indicate potential roles in yield loss under heat stress. Many of these genes have only recently been characterized in potato, and the majority of them have not been studied in the context of elevated temperature. Additionally, the patterns I observed in expression of FT subfamily versus TFL subfamily genes suggest other factors are responsible for upstream regulation/activation of these genes; transcription factors such ones in the BEL1 family are

known to be responsible for at least SP6A activation (Sharma et al. 2016). More research exploring the regulatory mechanisms of the PEBP family could offer promising results in understanding heat resistance in potato.

Chapter 3: Conclusion

The expected rise in global temperatures in coming decades poses an impending threat to the production of many staple crops, especially ones that are as susceptible to heat stress as *S. tuberosum*. Understanding the effects of abiotic stress on crop plants is thus a crucial goal for coping with climate change. Here, I present an investigation of the mechanisms of potato yield loss under heat stress using a realistic future climate projection and a whole-plant approach of study. I measured physiological aspects as well as transcriptomics and endogenous phytohormone levels of potato plants grown under chronic ElevT. Transcriptomic analyses of leaves and tubers of different sizes revealed changes in storage protein metabolism under ElevT, possibly due to internal signaling pathways. I identified auxin and ABA to have potential roles in tuberization signaling under ElevT, as well as several prospective genes that may contribute to decreased sink strength of tubers. These genes include CEN and TOC1, which are known inhibitors of SP6A, as well as several other flowering genes that share similarities with SP6A as part of the PEBP gene family. It could benefit future studies to further investigate these genes under the context of temperature, as some prove to be promising candidate genes for breeding heat tolerance in potato.

References

Abelenda, J. A., Bergonzi, S., Oortwijn, M., Sonnewald, S., Du, M., Visser, R. G. F., Sonnewald, U., & Bachem, C. W. B. (2019). Source-Sink Regulation Is Mediated by Interaction of an FT Homolog with a SWEET Protein in Potato. *Current Biology: CB*, *29*(7), 1178–1186.e6.

Abelenda, J. A., Cruz-Oró, E., Franco-Zorrilla, J. M., & Prat, S. (2016). Potato StCONSTANS-like1 Suppresses Storage Organ Formation by Directly Activating the FT-like StSP5G Repressor. *Current Biology: CB*, *26*(7), 872–881.

Anders, S., Pyl, P. T., & Huber, W. (2015). HTSeq--a Python framework to work with high-throughput sequencing data. *Bioinformatics* , *31*(2), 166–169.

Andrews, S. 2010. FastQC: A Quality Control Tool for High Throughput Sequence Data [Online]. Available online at: http://www.bioinformatics.babraham.ac.uk/projects/fastqc/

Andy Robinson, Associate Professor and Extension Potato Agronomist, North Dakota State University/University of Minnesota Eugenia Banks, Potato Specialist, Ontario Potato Board. (2020). *Potato tuber second growth*. https://www.ag.ndsu.edu/publications/crops/potato-tuber-second-growth

Beals, K. A. (2019). Potatoes, Nutrition and Health. *American Journal of Potato Research: An Official Publication of the Potato Association of America*, *96*(2), 102–110.

Berardini, T. Z., Reiser, L., Li, D., Mezheritsky, Y., Muller, R., Strait, E., & Huala, E. (2015). The Arabidopsis information resource: Making and mining the "gold standard" annotated reference plant genome. *Genesis* , *53*(8), 474–485.

Bernal, J., Mouzo, D., López-Pedrouso, M., Franco, D., García, L., & Zapata, C. (2019). The Major Storage Protein in Potato Tuber Is Mobilized by a Mechanism Dependent on Its Phosphorylation Status. *International Journal of Molecular Sciences*, *20*(8). https://doi.org/10.3390/ijms20081889

Bian, Z., Gao, H., & Wang, C. (2020). NAC Transcription Factors as Positive or Negative Regulators during Ongoing Battle between Pathogens and Our Food Crops. *International Journal of Molecular Sciences*, *22*(1). https://doi.org/10.3390/ijms22010081

Birch, P. R. J., Bryan, G., Fenton, B., Gilroy, E. M., Hein, I., Jones, J. T., Prashar, A., Taylor, M. A., Torrance, L., & Toth, I. K. (2012). Crops that feed the world 8: Potato: are the trends of increased global production sustainable? *Food Security*, *4*(4), 477–508.

Bita, C. E., & Gerats, T. (2013). Plant tolerance to high temperature in a changing environment: scientific fundamentals and production of heat stress-tolerant crops. *Frontiers in Plant Science*, *4*, 273.

Chen, P., Yang, R., Bartels, D., Dong, T., & Duan, H. (2022). Roles of Abscisic Acid and Gibberellins in Stem/Root Tuber Development. *International Journal of Molecular Sciences*, *23*(9). https://doi.org/10.3390/ijms23094955

Chen, S., Zhou, Y., Chen, Y., & Gu, J. (2018). fastp: an ultra-fast all-in-one FASTQ preprocessor. *Bioinformatics* , *34*(17), i884–i890.

Dahal, K., Li, X.-Q., Tai, H., Creelman, A., & Bizimungu, B. (2019). Improving Potato Stress Tolerance and Tuber Yield Under a Climate Change Scenario - A Current Overview. *Frontiers in Plant Science*, *10*, 563.

Da Ros, L., Elferjani, R., Soolanayakanahally, R., Kagale, S., Pahari, S., Kulkarni, M., Wahab, J., & Bizimungu, B. (2020). Drought-Induced Regulatory Cascades and Their Effects on

the Nutritional Quality of Developing Potato Tubers. *Genes*, *11*(8). https://doi.org/10.3390/genes11080864

de Haan, S., & Rodriguez, F. (2016). Chapter 1 - Potato Origin and Production. In J. Singh & L. Kaur (Eds.), *Advances in Potato Chemistry and Technology (Second Edition)* (pp. 1–32). Academic Press.

Dutt, S., Manjul, A. S., Raigond, P., Singh, B., Siddappa, S., Bhardwaj, V., Kawar, P. G., Patil, V. U., & Kardile, H. B. (2017). Key players associated with tuberization in potato: potential candidates for genetic engineering. *Critical Reviews in Biotechnology*, *37*(7), 942–957.

Dutta, M., Raturi, V., Gahlaut, V., Kumar, A., Sharma, P., Verma, V., Gupta, V. K., Sood, S., & Zinta, G. (2022). The interplay of DNA methyltransferases and demethylases with tuberization genes in potato (Solanum tuberosum L.) genotypes under high temperature. *Frontiers in Plant Science*, *13*, 933740.

FAO. (2000). *Faostat: FAO Statistical Databases*. Food & Agriculture Organization of the United Nations (FAO). https://www.fao.org/faostat/en/#data/QCL/visualize

Galmés, J., Ochogavía, J. M., Gago, J., Roldán, E. J., Cifre, J., & Conesa, M. À. (2013). Leaf responses to drought stress in Mediterranean accessions of Solanum lycopersicum: anatomical adaptations in relation to gas exchange parameters. *Plant, Cell & Environment*, *36*(5), 920–935.

Ghelis, T., Bolbach, G., Clodic, G., Habricot, Y., Miginiac, E., Sotta, B., & Jeannette, E. (2008). Protein tyrosine kinases and protein tyrosine phosphatases are involved in abscisic acid-dependent processes in Arabidopsis seeds and suspension cells. *Plant Physiology*, *148*(3), 1668–1680.

Gibb, M., Kisiala, A. B., Morrison, E. N., & Emery, R. J. N. (2020). The Origins and Roles of Methylthiolated Cytokinins: Evidence From Among Life Kingdoms. *Frontiers in Cell and Developmental Biology*, *8*, 605672.

Ginzberg, I., Barel, G., Ophir, R., Tzin, E., Tanami, Z., Muddarangappa, T., de Jong, W., & Fogelman, E. (2009). Transcriptomic profiling of heat-stress response in potato periderm. *Journal of Experimental Botany*, *60*(15), 4411–4421.

Guo, M., Liu, J.-H., Ma, X., Luo, D.-X., Gong, Z.-H., & Lu, M.-H. (2016). The Plant Heat Stress Transcription Factors (HSFs): Structure, Regulation, and Function in Response to Abiotic Stresses. *Frontiers in Plant Science*, *7*, 114.

Hameed, A., Zaidi, S. S.-E.-A., Shakir, S., & Mansoor, S. (2018). Applications of New Breeding Technologies for Potato Improvement. *Frontiers in Plant Science*, *9*, 925.

Hancock, R. D., Morris, W. L., Ducreux, L. J. M., Morris, J. A., Usman, M., Verrall, S. R., Fuller, J., Simpson, C. G., Zhang, R., Hedley, P. E., & Taylor, M. A. (2014). Physiological, biochemical and molecular responses of the potato (Solanum tuberosum L.) plant to moderately elevated temperature. *Plant, Cell & Environment*, *37*(2), 439–450.

Hannapel, D. J., Chen, H., Rosin, F. M., Banerjee, A. K., & Davies, P. J. (2004). Molecular controls of tuberization. *American Journal of Potato Research: An Official Publication of the Potato Association of America*, *81*(4), 263–274.

Hardigan, M. A., Laimbeer, F. P. E., Newton, L., Crisovan, E., Hamilton, J. P., Vaillancourt, B., Wiegert-Rininger, K., Wood, J. C., Douches, D. S., Farré, E. M., Veilleux, R. E., & Buell, C. R. (2017). Genome diversity of tuber-bearing *Solanum* uncovers complex evolutionary history and targets of domestication in the cultivated potato. *Proceedings of*

the National Academy of Sciences of the United States of America, *114*(46), E9999–E10008.
Hatfield, J. L., & Prueger, J. H. (2015). Temperature extremes: Effect on plant growth and development. *Weather and Climate Extremes*, *10*, 4–10.
Hoopes, G. M., Zarka, D., Feke, A., Acheson, K., Hamilton, J. P., Douches, D., Buell, C. R., & Farré, E. M. (2022). Keeping time in the dark: Potato diel and circadian rhythmic gene expression reveals tissue-specific circadian clocks. *Plant Direct*, *6*(7), e425.
IPCC, 2021: *Climate Change 2021: The Physical Science Basis. Contribution of Working Group I to the Sixth Assessment Report of the Intergovernmental Panel on Climate Change*[Masson-Delmotte, V., P. Zhai, A. Pirani, S.L. Connors, C. Péan, S. Berger, N. Caud, Y. Chen, L. Goldfarb, M.I. Gomis, M. Huang, K. Leitzell, E. Lonnoy, J.B.R. Matthews, T.K. Maycock, T. Waterfield, O. Yelekçi, R. Yu, and B. Zhou (eds.)]. Cambridge University Press, Cambridge, United Kingdom and New York, NY, USA, In press, doi:10.1017/9781009157896.
Jan, S., Abbas, N., Ashraf, M., & Ahmad, P. (2019). Roles of potential plant hormones and transcription factors in controlling leaf senescence and drought tolerance. *Protoplasma*, *256*(2), 313–329.
Janni, M., Gullì, M., Maestri, E., Marmiroli, M., Valliyodan, B., Nguyen, H. T., & Marmiroli, N. (2020). Molecular and genetic bases of heat stress responses in crop plants and breeding for increased resilience and productivity. *Journal of Experimental Botany*, *71*(13), 3780–3802.
Jia, L., Hao, K., Suyala, Q., Qin, Y., Yu, J., Liu, K., & Fan, M. (2022). Potato tuber degradation is regulated by carbohydrate metabolism: Results of transcriptomic analysis. *Plant Direct*, *6*(1), e379.
Jing, S., Jiang, P., Sun, X., Yu, L., Wang, E., Qin, J., Zhang, F., Prat, S., & Song, B. (2023). Long-Distance Control of Potato Storage Organ Formation by SELF PRUNING 3D and FLOWERING LOCUS T-like 1. *Plant Communications*, 100547.
Kim, D., Paggi, J. M., Park, C., Bennett, C., & Salzberg, S. L. (2019). Graph-based genome alignment and genotyping with HISAT2 and HISAT-genotype. *Nature Biotechnology*, *37*(8), 907–915.
Kloosterman, B., Navarro, C., Bijsterbosch, G., Lange, T., Prat, S., Visser, R. G. F., & Bachem, C. W. B. (2007). StGA2ox1 is induced prior to stolon swelling and controls GA levels during potato tuber development. *The Plant Journal: For Cell and Molecular Biology*, *52*(2), 362–373.
Kondhare, K. R., Kumar, A., Patil, N. S., Malankar, N. N., Saha, K., & Banerjee, A. K. (2021). Development of aerial and belowground tubers in potato is governed by photoperiod and epigenetic mechanism. *Plant Physiology*, *187*(3), 1071–1086.
Legnaioli, T., Cuevas, J., & Mas, P. (2009). TOC1 functions as a molecular switch connecting the circadian clock with plant responses to drought. *The EMBO Journal*, *28*(23), 3745–3757.
Lehretz, G. G., Sonnewald, S., Hornyik, C., Corral, J. M., & Sonnewald, U. (2019). Post-transcriptional Regulation of FLOWERING LOCUS T Modulates Heat-Dependent Source-Sink Development in Potato. *Current Biology: CB*, *29*(10), 1614–1624.e3.
Leisner, C. P., Potnis, N., & Sanz-Saez, A. (2022). Crosstalk and trade-offs: Plant responses to climate change-associated abiotic and biotic stresses. *Plant, Cell & Environment*. https://doi.org/10.1111/pce.14532

Leisner, C. P., Wood, J. C., Vaillancourt, B., Tang, Y., Douches, D. S., Robin Buell, C., & Winkler, J. A. (2017). Impact of choice of future climate change projection on growth chamber experimental outcomes: a preliminary study in potato. *International Journal of Biometeorology*, *62*(4), 669–679.

Li, C., & Robin Buell, C. (2022). 'Simple Tidy GeneCoEx': a gene co-expression analysis workflow powered by tidyverse and graph-based clustering in R. In *bioRxiv* (p. 2022.11.11.516131). https://doi.org/10.1101/2022.11.11.516131

Li, N., Euring, D., Cha, J. Y., Lin, Z., Lu, M., Huang, L.-J., & Kim, W. Y. (2020). Plant Hormone-Mediated Regulation of Heat Tolerance in Response to Global Climate Change. *Frontiers in Plant Science*, *11*, 627969.

Love, M. I., Huber, W., & Anders, S. (2014). Moderated estimation of fold change and dispersion for RNA-seq data with DESeq2. *Genome Biology*, *15*(12), 550.

Mäck, G., & Schjoerring, J. K. (2002). Effect of NO3 - supply on N metabolism of potato plants (Solanum tuberosum L.) with special focus on the tubers. *Plant, Cell & Environment*, *25*(8), 999–1009.

Morris, W. L., Ducreux, L. J. M., Morris, J., Campbell, R., Usman, M., Hedley, P. E., Prat, S., & Taylor, M. A. (2019). Identification of TIMING OF CAB EXPRESSION 1 as a temperature-sensitive negative regulator of tuberization in potato. *Journal of Experimental Botany*, *70*(20), 5703–5714.

National Agricultural Statistics Service (NASS). (2021). *North American Potatoes*. United States Department of Agriculture (USDA).

Navarro, C., Abelenda, J. A., Cruz-Oró, E., Cuéllar, C. A., Tamaki, S., Silva, J., Shimamoto, K., & Prat, S. (2011). Control of flowering and storage organ formation in potato by FLOWERING LOCUS T. *Nature*, *478*(7367), 119–122.

Obidiegwu, J. E., Bryan, G. J., Jones, H. G., & Prashar, A. (2015). Coping with drought: stress and adaptive responses in potato and perspectives for improvement. *Frontiers in Plant Science*, *6*, 542.

Park, J.-S., Park, S.-J., Kwon, S.-Y., Shin, A.-Y., Moon, K.-B., Park, J. M., Cho, H. S., Park, S. U., Jeon, J.-H., Kim, H.-S., & Lee, H.-J. (2022). Temporally distinct regulatory pathways coordinate thermo-responsive storage organ formation in potato. *Cell Reports*, *38*(13), 110579.

Pathak, A., & Upadhyaya, C. P. (2021). A Brief Insight on the Role of Various Phytohormones in Potato (Solanum tuberosum L) Tuber Development. In S. Hayat, H. Siddiqui, & C. A. Damalas (Eds.), *Salicylic Acid - A Versatile Plant Growth Regulator* (pp. 249–263). Springer International Publishing.

Patro, R., Duggal, G., Love, M. I., Irizarry, R. A., & Kingsford, C. (2017). Salmon provides fast and bias-aware quantification of transcript expression. *Nature Methods*, *14*(4), 417–419.

Pencík, A., Simonovik, B., Petersson, S. V., Henyková, E., Simon, S., Greenham, K., Zhang, Y., Kowalczyk, M., Estelle, M., Zazímalová, E., Novák, O., Sandberg, G., & Ljung, K. (2013). Regulation of auxin homeostasis and gradients in Arabidopsis roots through the formation of the indole-3-acetic acid catabolite 2-oxindole-3-acetic acid. *The Plant Cell*, *25*(10), 3858–3870.

Pham, G. M., Hamilton, J. P., Wood, J. C., Burke, J. T., Zhao, H., Vaillancourt, B., Ou, S., Jiang, J., & Buell, C. R. (2020). Construction of a chromosome-scale long-read reference genome assembly for potato. *GigaScience*, *9*(9). https://doi.org/10.1093/gigascience/giaa100

Prerostova, S., Dobrev, P. I., Knirsch, V., Jarosova, J., Gaudinova, A., Zupkova, B., Prášil, I. T., Janda, T., Brzobohatý, B., Skalák, J., & Vankova, R. (2021). Light Quality and Intensity Modulate Cold Acclimation in Arabidopsis. *International Journal of Molecular Sciences*, *22*(5). https://doi.org/10.3390/ijms22052736

R Core Team (2022). *R: A Language and Environment for Statistical Computing*. R Foundation for Statistical Computing, Vienna, Austria. https://www.R-project.org.

Rykaczewska, K. (2013). The impact of high temperature during growing season on potato cultivars with different response to environmental stresses. *American Journal of Plant Sciences*, *04*(12), 2386–2393.

Rykaczewska, K. (2015). The Effect of High Temperature Occurring in Subsequent Stages of Plant Development on Potato Yield and Tuber Physiological Defects. *American Journal of Potato Research: An Official Publication of the Potato Association of America*, *92*(3), 339–349.

Sade, N., Del Mar Rubio-Wilhelmi, M., Umnajkitikorn, K., & Blumwald, E. (2018). Stress-induced senescence and plant tolerance to abiotic stress. *Journal of Experimental Botany*, *69*(4), 845–853.

Sharma, P., Lin, T., & Hannapel, D. J. (2016). Targets of the StBEL5 Transcription Factor Include the FT Ortholog StSP6A. *Plant Physiology*, *170*(1), 310–324.

Singh, A., Siddappa, S., Bhardwaj, V., Singh, B., Kumar, D., & Singh, B. P. (2015). Expression profiling of potato cultivars with contrasting tuberization at elevated temperature using microarray analysis. *Plant Physiology and Biochemistry: PPB / Societe Francaise de Physiologie Vegetale*, *97*, 108–116.

Singh, B., Kukreja, S., & Goutam, U. (2020). Impact of heat stress on potato (Solanum tuberosum L.): present scenario and future opportunities. *The Journal of Horticultural Science & Biotechnology*, *95*(4), 407–424.

Solanaceae Genomic Resource. (n.d.). *Spud DB*. Retrieved January 20, 2023, from http://spuddb.uga.edu/

Sprenger, H., Kurowsky, C., Horn, R., Erban, A., Seddig, S., Rudack, K., Fischer, A., Walther, D., Zuther, E., Köhl, K., Hincha, D. K., & Kopka, J. (2016). The drought response of potato reference cultivars with contrasting tolerance. *Plant, Cell & Environment*, *39*(11), 2370–2389.

Sterrett, S. B., Henningre, M. R., & Lee, G. S. (1991). Relationship of Internal Heat Necrosis of Potato to Time and Temperature after Planting. *Journal of the American Society for Horticultural Science. American Society for Horticultural Science*, *116*(4), 697–700.

Tang, D., Jia, Y., Zhang, J., Li, H., Cheng, L., Wang, P., Bao, Z., Liu, Z., Feng, S., Zhu, X., Li, D., Zhu, G., Wang, H., Zhou, Y., Zhou, Y., Bryan, G. J., Buell, C. R., Zhang, C., & Huang, S. (2022). Genome evolution and diversity of wild and cultivated potatoes. *Nature*, *606*(7914), 535–541.

Tang, R., Niu, S., Zhang, G., Chen, G., Haroon, M., Yang, Q., Rajora, O. P., & Li, X.-Q. (2018). Physiological and growth responses of potato cultivars to heat stress. *Botany*, *96*(12), 897–912.

Teo, C. J., Takahashi, K., Shimizu, K., Shimamoto, K., & Taoka, K.-I. (2017). Potato Tuber Induction is Regulated by Interactions Between Components of a Tuberigen Complex. *Plant & Cell Physiology*, *58*(2), 365–374.

Thomas, P. D., Ebert, D., Muruganujan, A., Mushayahama, T., Albou, L.-P., & Mi, H. (2022). PANTHER: Making genome-scale phylogenetics accessible to all. *Protein Science: A Publication of the Protein Society*, *31*(1), 8–22.

Timlin, D., Lutfor Rahman, S. M., Baker, J., Reddy, V. R., Fleisher, D., & Quebedeaux, B. (2006). Whole plant photosynthesis, development, and carbon partitioning in potato as a function of temperature. *Agronomy Journal*, *98*(5), 1195–1203.

Umezawa, T., Sugiyama, N., Takahashi, F., Anderson, J. C., Ishihama, Y., Peck, S. C., & Shinozaki, K. (2013). Genetics and phosphoproteomics reveal a protein phosphorylation network in the abscisic acid signaling pathway in Arabidopsis thaliana. *Science Signaling*, *6*(270), rs8.

Van Dam, J., Kooman, P. L., & Struik, P. C. (1996). Effects of temperature and photoperiod on early growth and final number of tubers in potato (Solanum tuberosum L.). *Potato Research*, *39*(1), 51–62.

Wang, Z., Ma, R., Zhao, M., Wang, F., Zhang, N., & Si, H. (2020). NO and ABA Interaction Regulates Tuber Dormancy and Sprouting in Potato. *Frontiers in Plant Science*, *11*, 311.

Weeda, S. M., Mohan Kumar, G. N., & Richard Knowles, N. (2009). Developmentally linked changes in proteases and protease inhibitors suggest a role for potato multicystatin in regulating protein content of potato tubers. *Planta*, *230*(1), 73–84.

Wickham, H., Averick, M., Bryan, J., Chang, W., McGowan, L., François, R., Grolemund, G., Hayes, A., Henry, L., Hester, J., Kuhn, M., Pedersen, T., Miller, E., Bache, S., Müller, K., Ooms, J., Robinson, D., Seidel, D., Spinu, V., … Yutani, H. (2019). Welcome to the tidyverse. *Journal of Open Source Software*, *4*(43), 1686.

Wolf, S., Marani, A., & Rudich, J. (1990). Effects of Temperature and Photoperiod on Assimilate Partitioning in Potato Plants. *Annals of Botany*, *66*(5), 513–520.

Wu, T., Hu, E., Xu, S., Chen, M., Guo, P., Dai, Z., Feng, T., Zhou, L., Tang, W., Zhan, L., Fu, X., Liu, S., Bo, X., & Yu, G. (2021). clusterProfiler 4.0: A universal enrichment tool for interpreting omics data. *Innovation (Cambridge (Mass.))*, *2*(3), 100141.

Xu, X., van Lammeren, A. A. M., Vermeer, E., & Vreugdenhil, D. (1998). The Role of Gibberellin, Abscisic Acid, and Sucrose in the Regulation of Potato Tuber Formation in Vitro1. In *Plant Physiology* (Vol. 117, Issue 2, pp. 575–584). https://doi.org/10.1104/pp.117.2.575

Zaheer, K., & Akhtar, M. H. (2016). Potato Production, Usage, and Nutrition—A Review. *Critical Reviews in Food Science and Nutrition*, *56*(5), 711–721.

Zhang, C., Wang, P., Tang, D., Yang, Z., Lu, F., Qi, J., Tawari, N. R., Shang, Y., Li, C., & Huang, S. (2019). The genetic basis of inbreeding depression in potato. *Nature Genetics*, *51*(3), 374–378.

Zhang, G., Jin, X., Li, X., Zhang, N., Li, S., Si, H., Rajora, O. P., & Li, X.-Q. (2021a). Genome-wide identification of PEBP gene family members in potato and their phylogenetic relationships and expression patterns under heat stress. In *Research Square*. https://doi.org/10.21203/rs.3.rs-809879/v1

Zhang, G., Tang, R., Niu, S., Si, H., Yang, Q., Rajora, O. P., & Li, X.-Q. (2021b). Heat-stress-induced sprouting and differential gene expression in growing potato tubers: Comparative transcriptomics with that induced by postharvest sprouting. *Horticulture Research*, *8*(1), 226.

Zhang, X., Campbell, R., Ducreux, L. J. M., Morris, J., Hedley, P. E., Mellado-Ortega, E., Roberts, A. G., Stephens, J., Bryan, G. J., Torrance, L., Chapman, S. N., Prat, S., &

Taylor, M. A. (2020). TERMINAL FLOWER-1/CENTRORADIALIS inhibits tuberisation via protein interaction with the tuberigen activation complex. *The Plant Journal: For Cell and Molecular Biology*, *103*(6), 2263–2278.

Zhu, T., De Lima, C. F. F., & De Smet, I. (2021). The Heat is On: How Crop Growth, Development and Yield Respond to High Temperature. *Journal of Experimental Botany*. https://doi.org/10.1093/jxb/erab308

Zierer, W., Rüscher, D., Sonnewald, U., & Sonnewald, S. (2021). Tuber and Tuberous Root Development. *Annual Review of Plant Biology*, *72*, 551–580.

Zuo, Z.-F., He, W., Li, J., Mo, B., & Liu, L. (2021). Small RNAs: The Essential Regulators in Plant Thermotolerance. *Frontiers in Plant Science*, *12*, 726762.

Zwack, P. J., De Clercq, I., Howton, T. C., Hallmark, H. T., Hurny, A., Keshishian, E. A., Parish, A. M., Benkova, E., Mukhtar, M. S., Van Breusegem, F., & Rashotte, A. M. (2016). Cytokinin Response Factor 6 Represses Cytokinin-Associated Genes during Oxidative Stress. *Plant Physiology*, *172*(2), 1249–1258.

Appendix 1: Supplementary Material

Supplementary Material 1: Conviron Adaptis growth chamber settings

AmbT Temp: 1980-2000 average temps for each 2 week period from Eau Claire weather station
ElevT Temp: Used Tmin and Tmax from CRCM_cgcm3 model from Leisner et al. (2017)
Period 1-8: Mimic May-September (120 day growing season); each period is 2 weeks
Light: 300-500 µmol m−2 s−1
CO_2 levels: ambient

Period	Line	Time	AmbT Temp (°C)	ElevT Temp (°C)	RH (%)	Light (0-3)	Photoperiod
1	1	6:00	11.1	13.8	60	1	14 hr 51 min
	2	6:30	11.5	14.1	60	2	
	3	7:00	11.9	14.5	60	3	
	4	9:30	14	15.1	60	3	
	5	13:00	17	18.8	60	3	
	6	17:00	20.5	21.7	60	3	
	7	19:51	23	23.78	60	3	
	8	20:11	22.4	23.3	60	2	
	9	20:31	21.8	22.7	60	1	
	10	20:51	21.4	22.5	60	0	
	11	23:00	19.25	20.4	60	0	
	12	1:30:00	17.8	18.9	60	0	
	13	4:00	14.2	15.7	60	0	
2	1	6:00	13.68	15.91	60	1	15 hr 16 min
	2	6:30	14	16.31	60	2	
	3	7:00	14.5	16.7	60	3	
	4	9:30	16.5	18.7	60	3	
	5	13:00	19.44	21.5	60	3	
	6	17:00	22.7	24.7	60	3	
	7	20:16	25.42	27.31	60	3	
	8	20:36	24.8	26.7	60	2	
	9	20:56	24.2	26.1	60	1	
	10	21:16	23.8	25.7	60	0	
	11	23:00	21.8	23.8	60	0	
	12	1:30:00	18.8	20.9	60	0	
	13	4:00	15.8	17.9	60	0	
3	1	6:00	15.9	18.13	60	1	15 hr 22 min
	2	6:30	16.3	18.5	60	2	

	3	7:00	16.7	18.9	60	3	
	4	9:30	18.8	20.9	60	3	
	5	13:00	21.6	23.7	60	3	
	6	17:00	24.9	26.9	60	3	
	7	20:22	27.68	29.57	60	3	
	8	20:42	27.1	29	60	2	
	9	21:02	26.4	28.4	60	1	
	10	21:22	26	28	60	0	
	11	23:00	24	26	60	0	
	12	1:30:00	20.9	23	60	0	
	13	4:00	17.9	20	60	0	
4	1	6:00	17.37	20.72	60	1	15 hr 13 min
	2	6:30	17.8	21.2	60	2	
	3	7:00	18.2	21.6	60	3	
	4	9:30	20.1	23.8	60	3	
	5	13:00	23	26.8	60	3	
	6	17:00	26.1	30.2	60	3	
	7	20:13	28.72	33.03	60	3	
	8	20:33	28.1	32.4	60	2	
	9	20:53	27.6	31.8	60	1	
	10	21:13	27.2	31.4	60	0	
	11	23:00	25.2	29.3	60	0	
	12	1:30:00	22.3	26.1	60	0	
	13	4:00	19.4	23	60	0	
5	1	6:00	17.78	21.12	60	1	14 hr 50 min
	2	6:30	18.2	21.5	60	2	
	3	7:00	18.6	22	60	3	
	4	9:30	20.5	24.1	60	3	
	5	13:00	23.3	27.1	60	3	
	6	17:00	26.4	30.5	60	3	
	7	19:50	28.59	32.91	60	3	
	8	20:10	28.2	32.5	60	2	
	9	20:30	27.9	32.1	60	1	
	10	20:50	27.5	31.8	60	0	
	11	23:00	25.4	29.4	60	0	
	12	1:30:00	22.7	26.5	60	0	
	13	4:00	20.1	23.6	60	0	
6	1	6:00	17.06	20.19	60	1	14 hr 17 min
	2	6:30	17.5	20.6	60	2	

	3	7:00	17.9	21.1	60	3	
	4	9:30	19.9	23.4	60	3	
	5	13:00	22.7	26.6	60	3	
	6	17:00	25.9	30.3	60	3	
	7	19:17	27.77	32.35	60	3	
	8	19:37	27.4	32	60	2	
	9	19:57	27.1	31.6	60	1	
	10	20:17	26.8	31.2	60	0	
	11	23:00	24.8	28.9	60	0	
	12	1:30:00	22.3	26.1	60	0	
	13	4:00	19.8	23.3	60	0	
7	1	6:00	16.54	19.67	60	1	13 hr 37 min
	2	6:30	17	20.1	60	2	
	3	7:00	17.4	20.6	60	3	
	4	9:30	19.5	23	60	3	
	5	13:00	22.4	26.3	60	3	
	6	17:00	25.7	30.1	60	3	
	7	18:37	27.09	31.67	60	3	
	8	18:57	26.8	31.3	60	2	
	9	19:17	26.5	31	60	1	
	10	19:37	26.2	30.6	60	0	
	11	23:00	24.3	28.5	60	0	
	12	1:30:00	22	25.9	60	0	
	13	4:00	19.7	23.2	60	0	
8	1	6:00	14.59	17.01	60	1	12 hr 54 min
	2	6:30	15	17.5	60	2	
	3	7:00	15.5	18	60	3	
	4	9:30	17.7	20.3	60	3	
	5	13:00	20.9	23.7	60	3	
	6	17:00	24.5	27.5	60	3	
	7	17:54	25.27	28.32	60	3	
	8	18:14	25.1	28	60	2	
	9	18:34	24.9	27.7	60	1	
	10	18:54	24.5	27.4	60	0	
	11	23:00	22.8	25.5	60	0	
	12	1:30:00	20.6	23.2	60	0	
	13	4:00	18.3	20.8	60	0	

A. 

B. 

C. 

Supplementary Figure 1. Photographs of tuber initials (A), intermediate tubers (B), and mature tubers (C) collected from AmbT chamber 1 at 60d.

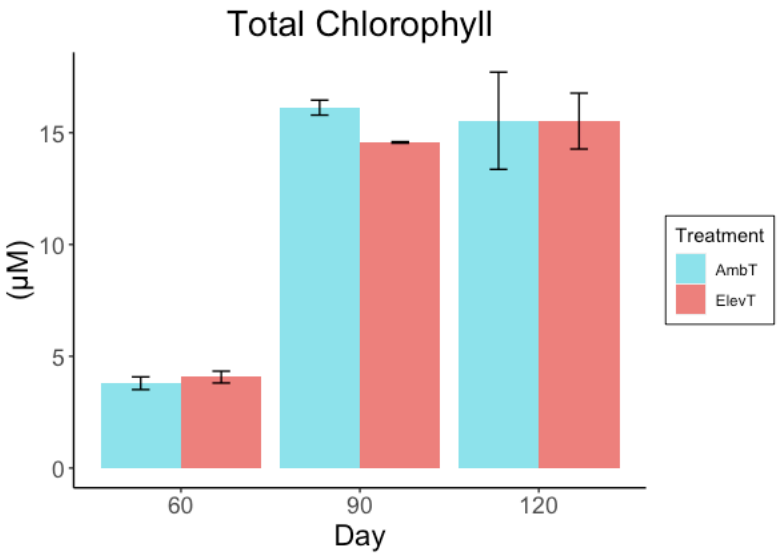

Supplementary Figure 2. Total chlorophyll (µM) averaged per four 6mm leaf discs collected from 60, 90, and 120d old plants. Error bars indicate standard error between biological replicates ($n = 2$). Pairwise *T*-tests were completed between treatments at each time point; no significant differences were found between AmbT and ElevT.

Supplementary Figure 3. Tuber initials collected from AmbT (left) and ElevT (right) plants at 30d. Stolons that displayed green coloring were removed and excluded from RNA and hormone analyses.

Sequencing Name	Treatment	Tissue Type	Time point	Total Input Reads	Total Input Read Pairs	Read Pairs After Trimming	% Reads Mapped
POT_AA	AmbT	Leaf	30d	41067802	20533901	20410699	90.99%
POT_AB	AmbT	Leaf	30d	45709502	22854751	22738906	91.21%
POT_AC	ElevT	Leaf	30d	46169230	23084615	22956639	90.70%
POT_AD	ElevT	Leaf	30d	39792536	19896268	19793455	90.90%
POT_AE	AmbT	TI	30d	44039020	22019510	21884005	89.90%
POT_AF	ElevT	TI	30d	39576566	19788283	19676707	90.45%
POT_AG	ElevT	TI	30d	48088194	24044097	23924142	89.61%
POT_AH	AmbT	Leaf	60d	39837204	19918602	19824747	89.66%
POT_AI	AmbT	Leaf	60d	48248350	24124175	24011354	90.05%
POT_AJ	ElevT	Leaf	60d	50036802	25018401	24891786	89.42%
POT_AK	ElevT	Leaf	60d	45946078	22973039	22877195	73.81%
POT_AL	AmbT	TI	60d	42034418	21017209	20931752	89.50%
POT_AM	AmbT	IMT	60d	45293156	22646578	22515844	89.12%
POT_AN	AmbT	MAT	60d	46211032	23105516	22996243	87.17%
POT_AO	AmbT	TI	60d	42260244	21130122	21030208	89.58%
POT_AP	AmbT	IMT	60d	46418996	23209498	23052161	88.96%
POT_AQ	AmbT	MAT	60d	43437888	21718944	21606858	87.24%

POT_AR	ElevT	TI	60d	46944200	23472100	23336708	89.83%
POT_AS	ElevT	IMT	60d	42318464	21159232	21060251	89.50%
POT_AT	ElevT	MAT	60d	47111984	23555992	23455407	88.52%
POT_AU	ElevT	TI	60d	50639716	25319858	25184919	88.46%
POT_AV	ElevT	IMT	60d	56008758	28004379	27861943	87.96%
POT_AW	ElevT	MAT	60d	46529702	23264851	23170239	87.33%
POT_AX	AmbT	Leaf	90d	40354622	20177311	20087789	86.26%
POT_AY	AmbT	Leaf	90d	47158890	23579445	23437219	89.50%
POT_AZ	ElevT	Leaf	90d	39389658	19694829	19573729	89.35%
POT_BA	ElevT	Leaf	90d	48492648	24246324	24124825	70.87%
POT_BB	AmbT	TI	90d	41967400	20983700	20893858	89.02%
POT_BC	AmbT	IMT	90d	40119170	20059585	19949441	88.60%
POT_BD	AmbT	MAT	90d	46740618	23370309	23277361	87.27%
POT_BE	AmbT	TI	90d	39172590	19586295	19479631	89.63%
POT_BF	AmbT	MAT	90d	40632950	20316475	20216937	86.98%
POT_BG	ElevT	TI	90d	45868556	22934278	22823500	89.24%
POT_BH	ElevT	TI	90d	41842696	20921348	20810272	88.04%
POT_BI	ElevT	IMT	90d	40369234	20184617	20080054	88.12%
POT_BJ	AmbT	Leaf	120d	46903702	23451851	23342325	76.83%
POT_BK	AmbT	Leaf	120d	49727416	24863708	24760327	66.98%
POT_BL	ElevT	Leaf	120d	42246252	21123126	21010826	90.09%
POT_BM	ElevT	Leaf	120d	41979778	20989889	20881975	62.48%
POT_BN	AmbT	TI	120d	40199814	20099907	19982364	87.59%
POT_BO	AmbT	IMT	120d	40910266	20455133	20370375	88.39%
POT_BP	AmbT	MAT	120d	45367876	22683938	22571283	86.64%
POT_BQ	AmbT	TI	120d	40248046	20124023	20017201	88.21%
POT_BR	AmbT	MAT	120d	42976846	21488423	21376345	87.26%
POT_BS	ElevT	TI	120d	48701122	24350561	24243231	89.28%
POT_BT	ElevT	MAT	120d	45355352	22677676	22541077	87.72%
POT_BU	ElevT	TI	120d	43583258	21791629	21663544	89.41%
POT_BV	ElevT	IMT	120d	59221960	29610980	29405255	88.47%
POT_BW	ElevT	MAT	120d	42212160	21106080	20962104	88.01%

Supplementary Table 1. RNA-sequencing read counts and alignment quality for 49 sequenced libraries. Metadata for treatment, tissue, and time point is also shown for each library. Reads were aligned to the doubled monoploid (DM) 1-3 516 R44 v6.1 *Solanum tuberosum* genome from SpudDB using HISAT (v2.2.1; Kim et al. 2019), and the alignment was annotated using the DM_1-3_516_R44_potato.v6.1.hc_gene_models.gff3 (downloaded Sept. 2022 from http://spuddb.uga.edu).

Sample	IAA	IAA-Asp	IAA-Glu	2,4-D	OxIAA	IAM	OxIAA-GE	I3A	ILacA	OxIAA-Glu	OxIAA-Asp
Leaf_90d_AmbT	496.32	50.61	0.32	1.09	359.03	91.82	2.87	588.08	19.43	23.51	2473.62
Leaf_90d_AmbT	407.83	28.66	0.56	1.06	314.25	140.29	5.63	575.17	38.93	16.60	1931.14
Leaf_90d_ElevT	306.96	25.29	0.73	0.83	136.85	115.75	4.78	613.35	16.90	11.83	1170.58
Leaf_90d_ElevT	221.51	42.10	0.64	0.16	160.42	148.46	5.68	295.19	11.40	14.20	1649.42
TI_90d_AmbT	116.19	0.00	0.00	20.86	31.78	11.66	9.05	320.33	13.86	2.77	4609.58
TI_90d_AmbT	162.20	0.00	0.00	60.65	25.82	7.18	4.76	208.74	18.17	2.92	2319.81
TI_90d_ElevT	412.07	0.00	0.00	33.73	53.10	20.52	8.54	1037.30	26.34	6.60	7383.57
TI_90d_ElevT	917.16	11.09	0.00	44.70	101.02	51.77	9.66	2025.89	28.03	6.70	5055.74
IMT_90d_AmbT	47.76	0.00	0.48	7.87	16.90	1.70	1.64	47.87	3.37	1.81	422.86
IMT_90d_ElevT	103.61	0.00	0.00	1.33	19.45	5.25	7.62	114.24	8.93	2.65	1213.93
MAT_90d_AmbT	155.50	6.52	0.52	8.09	42.23	7.87	2.13	152.82	2.18	2.96	210.05
MAT_90d_AmbT	81.63	4.16	0.32	2.89	35.11	3.18	3.72	84.56	2.32	3.34	210.79
Leaf_120d_AmbT	494.06	29.85	0.77	2.49	320.91	233.31	7.96	867.09	17.83	23.21	2493.05
Leaf_120d_AmbT	1440.44	154.80	0.65	1.74	292.10	877.33	9.99	2146.73	14.53	21.92	2152.90
Leaf_120d_ElevT	365.74	29.27	0.46	0.91	181.97	147.28	6.82	511.76	12.49	16.79	1046.33
Leaf_120d_ElevT	423.50	91.66	1.06	31.28	105.39	224.58	3.65	873.52	14.74	14.89	1288.36
TI_120d_AmbT	145.93	0.00	0.00	1024.56	50.44	14.98	9.45	444.43	39.39	4.31	5148.31
TI_120d_AmbT	190.79	0.00	0.00	2257.48	36.57	19.53	9.29	477.30	41.09	3.21	3777.83
TI_120d_ElevT	203.98	19.24	0.00	1.91	48.86	13.37	13.50	525.02	24.11	2.80	1162.11
TI_120d_ElevT	151.88	3.22	0.00	3.61	25.06	11.88	6.58	461.53	20.08	2.78	3903.36
MAT_120d_AmbT	183.99	6.19	0.47	328.31	31.60	11.67	1.73	139.86	2.43	2.86	203.11
MAT_120d_AmbT	237.54	10.60	0.50	3.87	60.79	16.87	1.17	413.13	5.83	3.13	255.22
MAT_120d_ElevT	235.75	13.66	0.78	12.91	32.93	11.29	8.83	282.88	14.17	17.15	315.66
MAT_120d_ElevT	273.75	10.20	0.80	2.70	48.75	15.19	3.93	390.12	9.84	3.48	281.66
IMT_120d_AmbT	214.62	0.00	0.00	468.08	31.92	7.28	2.83	160.41	6.83	2.49	643.52
IMT_120d_ElevT	118.72	0.00	0.00	10.30	28.31	7.33	7.92	316.17	35.70	5.74	2798.27

Supplementary Table 2a. Endogenous hormone levels in pmol/gDW of all auxin metabolites from 90d and 120d tissue samples as measured by liquid chromatography and mass spectrometry (LC/MS). Values are the average of three technical replicates per sample; replicates with a relative standard deviation higher than 30% were excluded from the average.

Sample	tZ	tZR	tZ7G	tZROG	tZRMP	DZR	DZ7G	DZ9G	cZR	cZ7G	cZ9G	cZOG	cZROG	cZRMP	iP	iPR	iP7G	iP9G	iPRMP	MeS-Z	MeS-ZR	MeS-iP	MeS-iPR
Leaf_90d_AmbT	14.73	2.07	137.66	2.11	1.20	1.82	23.56	1.77	2.04	173.57	1.19	1.30	11.11	1.95	0.47	14.36	952.95	2.80	2.05	0.83	110.09	1.06	0.35
Leaf_90d_AmbT	11.03	1.30	135.10	8.65	0.17	1.23	22.88	4.21	1.61	219.79	0.99	4.06	6.67	1.62	0.00	16.66	859.31	4.24	0.91	0.48	112.11	1.44	0.77
Leaf_90d_ElevT	36.33	1.09	159.95	3.84	0.99	3.32	24.26	2.77	1.63	339.96	1.90	5.00	7.30	1.51	3.50	15.03	1056.35	3.95	2.25	0.89	122.70	0.78	1.34
Leaf_90d_ElevT	10.62	0.62	350.97	15.24	0.68	1.06	57.37	9.78	1.93	932.10	4.80	30.71	16.70	2.46	0.00	21.98	2074.92	8.39	3.34	0.66	211.80	1.16	1.11
TI_90d_AmbT	17.28	7.19	128.84	6.91	1.35	1.40	52.22	0.36	9.94	408.38	45.54	11.23	13.40	6.33	4.24	25.94	1334.55	69.06	3.98	1.20	21.85	0.86	0.73
TI_90d_AmbT	15.20	25.16	110.44	9.35	1.28	2.56	59.65	0.13	13.35	271.64	23.76	7.17	10.56	0.97	2.00	30.14	816.42	27.80	0.81	0.85	15.28	0.65	0.17
TI_90d_ElevT	16.96	24.94	348.24	16.62	0.22	2.53	72.66	0.80	7.76	764.33	59.43	16.23	28.67	2.17	2.59	30.18	1636.34	58.38	1.42	1.31	26.60	1.47	1.95
TI_90d_ElevT	39.32	15.05	599.63	35.11	0.74	4.50	225.27	0.76	16.46	727.85	52.21	12.31	28.51	2.17	2.52	47.56	2476.43	62.53	1.83	0.99	54.33	1.76	1.75
IMT_90d_AmbT	6.08	20.42	78.87	5.00	2.14	0.77	22.68	0.47	5.87	109.42	5.99	3.72	7.30	6.96	1.20	22.96	514.03	5.53	8.65	0.62	5.40	0.54	0.30
IMT_90d_ElevT	15.24	72.04	167.21	19.88	4.06	5.89	81.64	0.45	14.14	160.39	6.18	4.94	20.58	7.43	1.20	53.03	608.42	7.15	4.04	0.92	12.31	1.15	0.47
MAT_90d_AmbT	6.42	51.95	46.95	9.08	10.18	2.02	17.16	0.28	12.53	49.06	1.73	2.15	9.16	20.87	2.00	51.69	402.86	1.56	21.39	0.52	7.03	0.76	0.60
MAT_90d_AmbT	10.54	36.30	32.39	7.05	4.43	2.16	18.04	0.24	12.00	37.24	1.58	1.64	7.07	21.10	2.05	49.69	314.76	2.83	26.34	0.55	7.29	0.73	0.53
Leaf_120d_AmbT	23.24	6.29	253.52	9.48	0.71	6.78	58.00	2.75	2.66	313.14	1.89	1.50	12.55	2.65	0.13	50.45	1352.19	6.12	4.71	1.43	54.63	1.63	2.56
Leaf_120d_AmbT	21.54	2.79	780.56	17.34	0.76	2.43	99.09	4.80	2.06	1028.80	6.21	27.49	28.24	3.89	3.88	22.50	3423.80	13.92	1.93	1.60	252.62	1.83	0.46
Leaf_120d_ElevT	33.06	21.39	251.30	9.78	0.35	5.51	41.07	2.92	2.01	352.33	1.67	3.84	9.56	1.10	0.67	12.48	1297.92	6.19	2.56	0.69	256.82	2.18	0.70
Leaf_120d_ElevT	21.65	9.44	234.73	10.13	1.14	21.60	60.22	6.18	1.97	438.79	2.64	10.54	8.83	3.56	0.00	13.15	1465.21	3.73	1.87	1.72	99.61	1.00	4.21
TI_120d_AmbT	16.67	9.45	163.28	7.91	1.97	4.60	94.43	2.60	7.09	627.57	110.71	14.89	29.76	6.03	3.78	10.21	1336.41	114.28	2.35	1.61	30.60	1.73	0.83
TI_120d_AmbT	10.52	8.60	221.84	4.15	0.31	1.71	89.23	2.40	5.98	642.13	98.61	9.36	21.96	4.16	7.79	9.51	2210.29	143.64	3.29	2.33	29.23	0.97	2.81
TI_120d_ElevT	11.12	9.88	383.56	17.17	5.86	2.39	153.81	0.29	10.82	541.83	48.55	7.01	25.35	12.67	3.16	16.40	2523.86	70.19	6.07	0.86	20.37	0.87	0.45
TI_120d_ElevT	12.37	13.41	248.36	15.78	3.14	2.03	118.21	0.14	5.15	466.45	43.24	10.10	22.63	11.85	3.07	21.88	1450.66	61.77	14.64	1.55	21.41	2.05	0.90
MAT_120d_AmbT	5.30	67.71	47.52	8.58	5.61	3.38	34.51	0.02	13.67	68.07	2.65	2.69	9.71	16.91	1.21	45.92	491.52	2.74	13.89	0.76	8.01	0.65	0.56
MAT_120d_AmbT	6.40	26.12	44.59	11.08	14.13	1.49	22.63	0.22	5.91	52.50	1.48	3.12	8.49	30.18	2.57	24.83	436.61	3.55	30.33	0.44	6.92	0.58	0.48
MAT_120d_ElevT	5.31	24.81	74.59	34.92	15.83	1.10	51.30	0.78	6.56	79.93	0.59	6.47	13.16	54.77	53.02	36.82	587.55	3.17	39.88	28.28	4.59	54.48	4.04
MAT_120d_ElevT	10.85	38.99	83.72	14.35	17.90	2.33	54.55	0.12	6.69	83.25	2.03	3.43	14.34	31.86	2.67	26.89	499.43	2.07	29.10	1.74	6.28	1.49	6.59
IMT_120d_AmbT	6.04	39.80	53.60	4.61	0.66	2.15	29.73	0.09	9.57	125.46	8.90	3.65	7.63	2.65	1.38	45.54	564.24	12.02	2.85	0.76	11.59	0.60	0.65
IMT_120d_ElevT	26.07	28.98	247.56	21.62	2.75	4.97	206.60	0.46	13.80	499.58	37.96	9.72	35.08	22.51	2.83	24.02	1024.89	38.81	13.60	2.25	16.23	2.63	3.14

Supplementary Table 2b. Endogenous hormone levels in pmol/gDW of all cytokinin metabolites from 90d and 120d tissue samples as measured by liquid chromatography and mass spectrometry (LC/MS). Values are the average of three technical replicates per sample; replicates with a relative standard deviation higher than 30% were excluded from the average.

Sample	ABA	ABA-GE	PA	DPA	9OH-ABA	JA	JA-Ile	cisOPDA	JA-Me	DiH-JA	dnOPDA	SA	BzA	PAA	PAAM	SinAc
Leaf_90d_AmbT	86.05	295.89	210.22	123.13	353.65	51.45	11.29	1258.49	1139.84	49.05	4001.83	2236.37	6256.11	12466.74	379.63	14.05
Leaf_90d_AmbT	212.86	515.03	273.54	245.01	252.48	99.03	26.03	4841.16	443.66	74.35	45735.90	959.32	10194.27	13920.06	617.78	13.68
Leaf_90d_ElevT	153.82	584.70	289.54	749.46	267.24	34.15	2.44	537.17	3398.74	96.49	2400.19	797.74	8910.73	11379.93	554.35	23.12
Leaf_90d_ElevT	77.35	647.45	144.62	508.51	133.48	51.80	5.96	734.54	1189.80	86.95	2165.13	1340.00	6439.28	5867.97	797.84	32.86
TI_90d_AmbT	89.08	3.73	126.71	313.00	116.95	287.23	214.94	105.23	1559.37	59.40	53.43	1057.35	18316.87	6511.12	122.58	8.82
TI_90d_AmbT	119.23	13.58	78.34	504.12	72.31	368.79	409.65	438.87	2165.78	44.27	104.95	1745.89	19538.19	9417.16	141.56	4.05
TI_90d_ElevT	27.26	54.35	85.82	351.79	79.21	263.98	93.41	580.59	1222.48	81.86	242.24	4210.96	29894.87	6064.10	156.71	14.00
TI_90d_ElevT	69.66	47.84	130.51	258.69	120.46	240.22	531.64	122.12	1295.05	89.11	460.31	5535.40	33296.74	6477.75	369.42	20.92
IMT_90d_AmbT	259.89	19.51	37.54	696.60	34.65	42.75	51.08	33.76	1387.25	31.77	79.65	360.46	9652.37	5881.83	45.52	2.87
IMT_90d_ElevT	90.09	65.71	95.81	1176.41	88.44	85.19	42.94	118.12	382.03	51.02	108.67	1460.11	15823.30	4599.72	128.37	13.62
MAT_90d_AmbT	195.52	9.39	86.39	1243.11	79.74	70.29	16.21	31.83	723.88	29.50	99.77	777.12	10914.63	8379.59	96.80	0.69
MAT_90d_AmbT	171.66	14.04	102.90	1357.17	94.98	56.89	7.67	119.98	257.13	39.54	54.04	869.03	12511.68	7053.33	77.18	0.57
Leaf_120d_AmbT	208.78	416.63	377.29	316.20	348.24	192.21	18.87	2030.61	286.90	120.29	7619.24	2068.08	21076.05	51286.98	1120.18	16.52
Leaf_120d_AmbT	279.27	1047.30	648.13	220.78	598.22	42.57	13.43	1738.33	454.45	153.70	1389.50	2382.31	14153.60	19337.48	2321.92	19.50
Leaf_120d_ElevT	66.71	757.67	250.32	454.72	231.05	120.00	16.49	1427.68	168.96	134.47	4750.79	1771.01	6723.25	8015.71	443.23	12.95
Leaf_120d_ElevT	150.63	503.84	212.81	525.99	196.43	106.81	3.64	1504.33	284.59	127.45	3692.30	2044.86	16127.16	22176.97	1647.99	14.01
TI_120d_AmbT	36.07	31.77	60.63	52.75	55.96	455.70	391.77	162.62	360.76	194.67	374.09	5347.44	30956.23	4396.69	206.06	24.19
TI_120d_AmbT	61.10	69.32	96.49	64.59	89.06	227.84	187.08	307.80	108.63	128.43	500.40	2853.51	26140.61	4521.86	152.30	15.39
TI_120d_ElevT	76.12	21.88	74.58	635.93	68.84	945.19	570.59	77.34	200.04	113.18	269.57	2418.30	26288.84	8200.83	249.07	17.98
TI_120d_ElevT	39.95	19.69	81.27	397.58	75.01	507.32	124.31	117.27	153.56	86.17	298.17	1429.95	21988.02	5003.70	179.51	22.24
MAT_120d_AmbT	249.91	22.13	99.81	1341.25	92.13	288.41	65.33	41.73	77.66	48.64	147.57	802.15	10358.06	5051.65	152.95	1.01
MAT_120d_AmbT	242.01	19.39	89.51	1351.82	82.62	226.27	25.97	56.90	49.82	43.17	178.19	880.14	14802.34	6566.97	138.43	1.15
MAT_120d_ElevT	159.66	0.00	75.65	2308.31	251.83	429.81	233.12	439.60	1033.92	121.30	11465.54	422.67	14555.92	9109.32	289.91	10.06
MAT_120d_ElevT	128.89	20.15	106.39	1472.92	98.20	481.59	87.05	158.22	201.61	52.77	429.21	943.86	20618.56	10505.43	137.44	3.36
IMT_120d_AmbT	177.46	18.61	189.50	910.10	174.90	436.66	113.44	55.75	54.62	60.56	52.26	1058.48	12140.85	4657.96	120.20	2.99
IMT_120d_ElevT	48.59	53.40	100.70	475.86	137.76	338.99	193.78	145.22	255.42	142.49	1144.32	3540.08	55896.92	5860.67	224.77	33.89

Supplementary Table 2c. Endogenous hormone levels in pmol/gDW of all abscisic acid (ABA, ABA-GE, PA, DPA, 9OH-ABA), jasmonic acid (JA, JA-Ile, cisOPDA, JA-Me, DiH-JA, dnOPDA), and phenolic compound (SA, BzA, PAA, PAAM, SinAc) metabolites from 90d and 120d tissue samples as measured by liquid chromatography and mass spectrometry (LC/MS). Values are the average of three technical replicates per sample; replicates with a relative standard deviation higher than 30% were excluded from the average.

Abbreviation	Full name
tZ	trans-Zeatin
tZR	trans-Zeatin riboside
tZ7G	trans-Zeatin-7-glucoside
tZROG	trans-Zeatin riboside -O-glucoside
tZRMP	trans-Zeatin riboside monophosphate
DZR	Dihydrozeatin riboside
DZ7G	Dihydrozeatin-7-glucoside
DZ9G	Dihydrozeatin-9-glucoside
cZR	cis-Zeatin riboside
cZ7G	cis-Zeatin-9-glucoside
cZ9G	cis-Zeatin-9-glucoside
cZOG	cis-Zeatin-O-glucoside
cZROG	cis-Zeatin riboside -O-glucoside
cZRMP	cis-Zeatin riboside monophosphate
iP	Isopentenyl adenine
iPR	Isopentenyl adenosine
iP7G	Isopentenyl adenine-7-glucoside
iP9G	Isopentenyl adenine-9-glucoside
iPRMP	Isopentenyl adenosine monophosphate
MeS-Z	2-methylthio zeatin
MeS-ZR	2-methylthio zeatin riboside
MeS-iP	2-methylthio isopentenyl adenosine
MeS-iPR	2-methylthio isopentenyl adenosine
ABA	Abscisic acid
ABA-GE	ABA-glucose ester
PA	Phaseic acid
DPA	Dihydrophaseic acid
9OH-ABA	9-hydroxy-ABA
NeoPA	Neophaseic acid
JA	Jasmonic acid
JA-Ile	JA-isoleucine
cisOPDA	cis-12-Oxo-Phytodienoic acid (JA precursor)
JA-Me	Jasmonic acid methyl ester
DiH-JA	dihydrojasmonic acid
dnOPDA	dinor OPDA
IAA	Indole-3-acetic acid
IAA-Asp	IAA-aspartate
IAA-Glu	IAA-glutamate
OxIAA	Oxo-IAA

OxIAA-Asp	Oxo-IAA-aspartate
OxIAA-GE	Oxo-IAA-glucose ester
I3A	Indole-3-aldehyde
ILacA	Indole-3-lactic acid
IAM	Indole-3-acetamide (IAA precursor)
2,4-D	2,4 dichlorophenoxyacetic acid (synthetic auxin)
SA	Salicylic acid
BzA	Benzoic acid
PAA	Phenylacetic acid
PAAM	Phenylacetamide
SinAc	Sinapic acid

Supplementary Table 2d. Abbreviations and full names of all metabolites measured by liquid chromatography and mass spectrometry (LC/MS) in the phytohormone analysis.

Gene IDs	Gene Name	Subfamily
Soltu.DM.01G007030.1	StPEBP3	TFL
Soltu.DM.03G011110.1	StSP3D	FT
Soltu.DM.11G004040.1	StFTL1	FT
Soltu.DM.05G024030.1	StSP5G-A	FT
Soltu.DM.01G006990.1	StPEBP2	TFL
Soltu.DM.09G008810.1	StPEBP12	PEBP-like
Soltu.DM.03G033490.1	StPEBP6	MFT
Soltu.DM.05G026370.1	StSP6A	FT
Soltu.DM.05G024040.1	StSP5G-B	FT
Soltu.DM.11G004050.1	StPEBP15	FT
Soltu.DM.09G008890.1	StPEBP13	PEBP-like
Soltu.DM.01G006970.1	StPEBP1	TFL
Soltu.DM.03G017110.1	StCEN	TFL
Soltu.DM.09G003550.1	StSP9D	TFL
Soltu.DM.06G029780.1	StPEBP10	TFL

Supplementary Table 3. Corresponding gene IDs of the phosphatidylethanolamine binding protein (PEBP) family genes, as well as their protein subfamily. Genes without set names in literature are referred to as StPEBP(1-15) as named in Zhang et al. (2022). Gene IDs correspond to the doubled monoploid (DM) 1-3 516 R44 v6.1 *Solanum tuberosum* genome from SpudDB (http://spuddb.uga.edu).